6228 J. Med. Chem. 2010, 53, 6228–6239
DOI: 10.1021/jm100639f

Journal of Medicinal Chemistry Article

Design, Synthesis, and Structure−Affinity Relationships of Regioisomeric *N*-Benzyl Alkyl Ether Piperazine Derivatives as σ-1 Receptor Ligands

Iman A. Moussa,[†] Samuel D. Banister,[†] Corinne Beinat,[†] Nicolas Giboureau,[‡,§] Aaron J. Reynolds,[†] and Michael Kassiou*[,†,‡,§]

[†]*School of Chemistry, and* [‡]*Discipline of Medical Radiation Sciences, University of Sydney, NSW 2006 Australia, and* [§]*Brain and Mind Research Institute, Sydney, NSW 2050 Australia*

Received May 26, 2010

A series of *N*-(benzofuran-2-ylmethyl)-*N*′-benzylpiperazines bearing alkyl or fluoroalkyl aryl ethers were synthesized and evaluated at various central nervous system receptors. Examination of in vitro σ_1 {[^{3}H](+)-pentazocine} and σ_2 ([^{3}H]DTG) receptor binding profiles of piperazines **11**−**13** and **25**−**36** revealed several highly potent and σ_1 selective ligands, notably, *N*-(benzofuran-2-ylmethyl)-*N*′-(4′-methoxybenzyl)piperazine (**13**, K_i = 2.7 nM, σ_2/σ_1 = 38) and *N*-(benzofuran-2-ylmethyl)-*N*′-(4′-(2″-fluoroethoxy)benzyl)piperazine (**30**, K_i = 2.6 nM, σ_2/σ_1 = 187). Structural features for optimal σ_1 receptor affinity and selectivity over the σ_2 receptor were identified. On the basis of its favorable log *D* value, **13** was selected as a candidate for the development of a σ_1 receptor positron emission tomography radiotracer. [^{11}C]**13** showed high uptake in the brain and other σ receptor-rich organs of a *Papio hamadryas* baboon. The in vivo evaluation of [^{11}C]**13** indicates that this radiotracer is a suitable candidate for imaging the σ_1 receptor in neurodegenerative processes.

Introduction

σ receptors were mistakenly identified as an opioid receptor subtype over 30 years ago.[1] The investigation of σ receptors with nonselective ligands led to a decade of confusion as σ receptors were erroneously reclassified as the phencyclidine/*N*-methyl-D-aspartate receptor complex.[2] Currently, σ receptors are recognized as a distinct class of mammalian protein, widely distributed in the central nervous system (CNS)[a] and peripheral organs, comprised of two pharmacologically well-defined subtypes: σ_1 and σ_2.[3] The σ_1 receptor has been cloned from numerous sources, including human brain tissue, and shows no similarity to any other mammalian protein.[4,5] Very recently, the σ_2 receptor was identified as a member of the histone protein family, but it has not been cloned.[6,7] Crystal structure data do not exist for either σ receptor subtype. An endogenous ligand for σ receptors has not been definitively identified; however, various neurosteroids, particularly progesterone, as well as the hallucinogenic trace amine, *N*,*N*-dimethyltryptamine (DMT), have been proposed to fulfill this role.[8−11]

It is believed that σ_1 receptors reside primarily at the interface between the endoplasmic reticulum (ER) and the mitochondrion, the mitochondria-associated ER membrane (MAM),[12] and modulate Ca^{2+} efflux from the ER by acting as molecular chaperones of inositol (1,4,5)-triphosphate receptors.[13,14] However, σ_1 receptors are also known to translocate to the plasma membrane where they regulate voltage-dependent Ca^{2+} channels and K^+ channels.[15−18] Much less is known about the nature of σ_2 signaling. Like σ_1 receptors,[19] the primary role of σ_2 receptors is thought to involve the maintenance of Ca^{2+} homeostasis.[20] Although σ receptors are linked to a variety of signaling pathways, the precise transduction mechanisms are complex and have not been fully elucidated. In the CNS, σ receptors are known to modulate several classical neurotransmitter systems, including those of acetylcholine,[21−23] dopamine,[24−27] glutamate,[28,29] 5-hydroxytryptamine,[30,31] and norepinephrine,[32−34] accounting for their implication in a diverse spectrum of CNS disorders.[35−37]

Initial interest in σ receptors as therapeutic targets was largely motivated by their high affinity for a range of clinically used typical antipsychotics, such as haloperidol (**1**, Figure 1).[38] The antipsychotic effect of functional antagonists of σ receptors is well-known, and several σ ligands have entered clinical trials for the treatment of schizophrenia.[39] Similarly, the finding that a number of structurally and pharmacologically diverse antidepressants, including fluvoxamine (**2**) and imipramine (**3**), also interact with σ receptors led to the investigation of σ receptors as a novel therapeutic target for the treatment of affective disorders.[40,41] Implication of σ receptors in anxiety and depression is widely accepted and has been comprehensively reviewed.[42−44] Widely abused psychostimulants, like cocaine (**4**) and methamphetamine (**5**), also interact with σ receptors at physiologically relevant concentrations, and it is believed that certain behavioral effects, addictive properties, and the toxicity of these drugs involve their activity at σ receptors.[45−49] Dozens of functional σ receptor antagonists have been shown to attenuate **4**-induced locomotor stimulation, convulsion, and lethality, thereby identifying σ receptors as an important target for the development of novel anti-**4** therapies.[46,47,49]

Numerous human tumor cell lines overexpress σ receptors,[50−52] and many σ ligands possess antiproliferative activity.[53−55] Indeed, σ_2 agonists have been shown to activate

*To whom correspondence should be addressed. Tel: +61-2-9351-0849. Fax: +61-2-9351-9146. E-mail: michael.kassiou@sydney.edu.au.

[a] Abbreviations: CNS, central nervous system; DMF, *N*,*N*-dimethylformamide; EDC·HCl, 1-ethyl-3-(3-dimethylaminopropyl)carbodiimide hydrochloride; ER, endoplasmic reticulum; HOBt, *N*-hydroxybenzotriazole; NMM, *N*-methylmorpholine; PET, positron emission tomography; RT, room temperature; TBAH, tetra-*n*-butylammonium hydroxide.

 Published on Web 07/28/2010

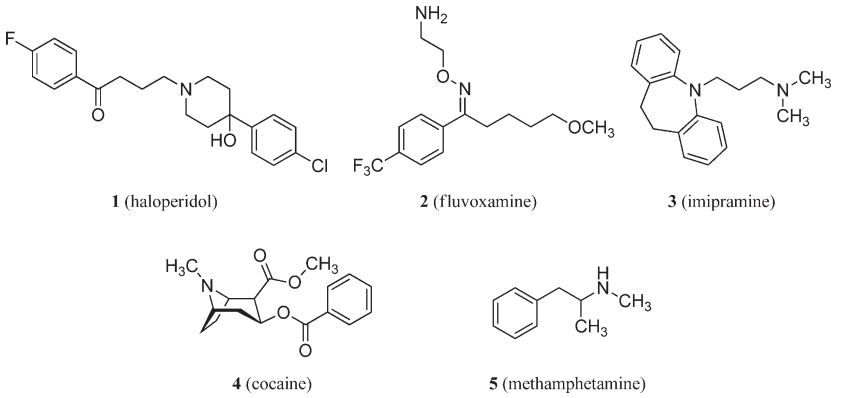

Figure 1. Examples of psychoactive drugs known to interact with σ receptors.

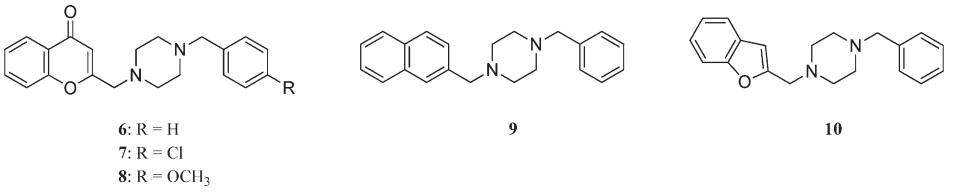

Figure 2. Examples of σ-selective arylalkyl piperazine ligands.

apoptosis and potentiate the effects of other antineoplastic agents.[56] Despite a limited understanding of the precise mechanistic role of σ receptors in cancer,[57] there is already much interest in σ receptors as cancer-associated biomarkers.[58] The design of selective σ ligands that are amenable to radiolabeling with carbon-11 or fluorine-18 would provide cancer imaging agents for use in the noninvasive technique, positron emission tomography (PET).[59]

The relative paucity of truly selective σ ligands, especially subtype-specific σ ligands, remains an impediment to σ receptor research. Consideration of the heterogeneity of known σ ligands underscores the difficulty of establishing a comprehensive σ receptor pharmacophore to aid the rational design of novel σ receptor probes. A model for σ_1 binding has been proposed; however, it is too simplistic to guide the rational design of high-affinity, selective σ_1 ligands.[60−63] Recently, several three-dimensional quantitative structure−activity relationship (3D-QSAR) analyses of σ_2 binding, each pertaining to a particular structural class of σ_2 ligands, were published.[64−66] The broad applicability and utility of these models to the rational design of selective σ ligands have not been demonstrated.

Work in our laboratory has focused on the development of increasingly selective σ ligands utilizing a polycarbocyclic scaffold, to elucidate the requisite structural features of σ receptor binding.[67] Additionally, we aim to develop σ ligands with potential therapeutic[68] and diagnostic applications. We report here the structure−affinity relationships of a series of novel arylalkyl piperazines as selective σ ligands and the development of a novel, carbon-11-labeled σ_1 ligand as a σ receptor imaging agent for use in PET.

The lead compound for this study was identified from a series of disubstituted 1,4-piperazines, flanked by a chromene ring and a benzyl group, reported by Baziard-Mouysset and co-workers.[69] The simplest member of this series, **6** (Figure 2), containing an unsubstituted benzyl ring, displayed high affinity for σ receptors (K_i = 3 nM) and negligible off-target activity ($5HT_{1A}$, $K_i > 10\,\mu M$; D_2, $K_i = 10\,\mu M$).[69] Substitution of the benzyl ring was generally detrimental to σ binding, with the exception of 4-chloro (**7**) or 4-methoxy substitution (**8**), which furnished improved σ ligands (K_i = 1 and 0.6 nM, respectively). By contrast, the chromene ring of **6** was shown to have little effect on σ binding, and substitution with a large number of alternate aromatic groups was well tolerated.[70] In particular, substitution with a naphthylmethyl (**9**) or 2-benzofurylmethyl group (**10**) conferred improved σ affinity (IC_{50} = 0.6 and 0.4 nM, respectively).[70] Unfortunately, no data are available regarding the subtype selectivity of the above compounds.

From the previously reported data, 4-methoxy substitution of the benzyl ring of **10** should be tolerated and could be expected to enhance σ affinity. Utilizing **10** as a lead compound, 2-, 3-, and 4-methoxybenzyl analogues were generated to explore the effect of aromatic substitution on σ receptor affinity and subtype selectivity. In addition to potential therapeutic activity, methoxy-substituted σ ligands would allow the development of ^{11}C-radiolabeled analogues for use as diagnostic probes in PET imaging in vivo.

To investigate the effect of steric augmentation of the benzyl substituent on σ receptor affinity and selectivity within this class, regioisomeric ethyl and propyl benzyl ethers were synthesized. To probe electronic factors influencing σ binding, a fluorine atom was introduced to the terminal position of the alkyl chain in both the ethyl and the propyl benzyl ether series. These compounds could also be labeled with fluorine-18 to enable further in vivo pharmacological evaluation.

Chemistry

Piperazines **10**−**13** were prepared according to the synthetic method shown in Scheme 1. Monoprotection of 1,4-piperazine (**14**) with di-*tert*-butyl dicarbonate gave rise to *N*-Boc piperazine (**15**).[71−73] Subjecting **15** to amide coupling with benzofuran-2-carboxylic acid gave **16**. Cleavage of the Boc protecting group under acidic conditions, to afford the hydrochloride salt **17**, was followed by aluminum hydride reduction to furnish amine **18** in 51% yield over four steps. Lead compound **10** and substituted methoxybenzyl piperazines **11**−**13** (identified as potential candidates for ^{11}C radiolabeling) were successfully

Scheme 1. Synthesis of *N*-Benzyl Piperazine Derivative **10** and *N*-(Methoxybenzyl) Piperazine Derivatives **11**−**13**[a]

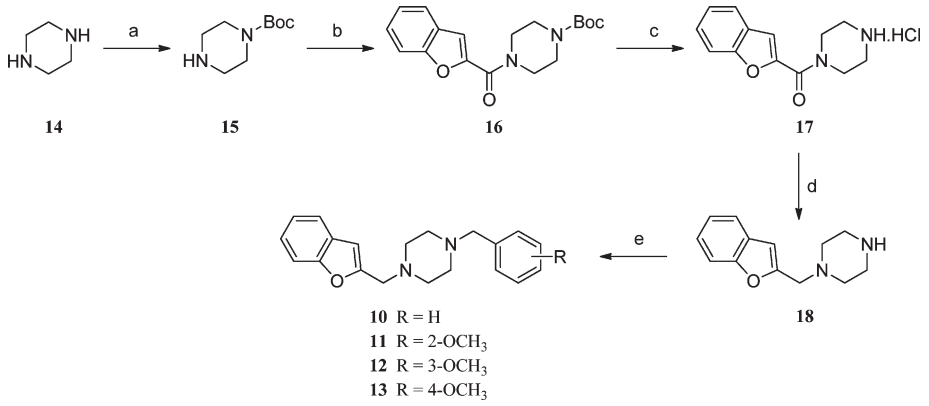

[a] Reagents and conditions: (a) Boc_2O, CH_2Cl_2, RT, 22 h, 81%. (b) Benzofuran-2-carboxylic acid, NMM, EDC · HCl, HOBt, DMF, RT, 20 h, 84%. (c) 4 M HCl in dioxane, RT, 0.5 h, quantitative. (d) AlH_3, 0 °C, 2 h, 75%. (e) Appropriate benzyl halide, K_2CO_3, NaI, DMF, reflux, 20 h, 81−84%.

Scheme 2. Synthesis of *N*-(Hydroxybenzyl) Piperazine Derivatives **19**−**21**[a]

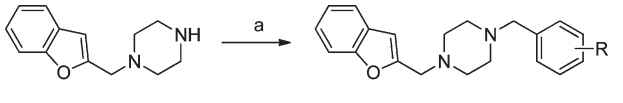

[a] Reagents and conditions: (a) Appropriate hydroxybenzaldehyde, $NaBH(OAc)_3$, $ClCH_2CH_2Cl$, RT, 4 h, 83−85%.

prepared from **18** by *N*-alkylation with the appropriate benzyl halides.

The desired ethers **25**−**33** could be prepared by alkylation of the appropriate regioisomeric phenolic precursors. Reductive amination of **18** with the appropriate hydroxybenzaldehyde in the presence of sodium triacetoxyborohydride provided the requisite phenols **19**−**21** in good yield and on a multigram scale (Scheme 2).

Alkylation of the regioisomeric phenols **19**−**21** with tosylates **22**−**24**, derived from ethanol, 2-fluoroethanol, and propanol, respectively, afforded the corresponding *N*-benzyl alkyl ether derivatives **25**−**33** (Scheme 3).

Similarly, the 2′-, 3′-, and 4′-(3″-fluoropropyl) benzyl ether derivatives **34**−**36** (Scheme 4) were prepared from the corresponding phenols **19**−**21** by alkylation with 3-fluoropropyl tosylate (**37**), accessible from commercially available 1,3-propanediol via monotosylation and deoxyfluorination.

Results and Discussion

Newly synthesized compounds **10**−**13** and **25**−**36** were subjected to in vitro binding assays against a comprehensive CNS receptor panel. K_i determinations and receptor binding profiles were provided by the National Institute of Mental Health's Psychoactive Drug Screening Program (NIMH PDSP). Affinities at σ_1 and σ_2 receptors were determined using a competitive modification of the protocol reported by Kovacs and Larson.[74] Competitive displacement of [^{3}H](+)-pentazocine in a rat brain homogenate preparation was used to determine σ_1 receptor affinity for all compounds screened. The affinity of test compounds for σ_2 receptors was determined by competitive displacement of [^{3}H]1,3-di-(2-tolyl)-guanidine ([^{3}H]DTG) from a PC12 cell preparation, a cell line known to overexpress σ_2 receptors, summarized in Tables 1−3.

The σ receptor affinity and subtype selectivity of unsubstituted lead structure **10** served as a point of comparison for the newly synthesized compounds, and several structure−activity relationship (SAR) trends were identified. Like parent compound **10**, most analogues within this series showed a distinct preference for the σ_1 receptor. Compounds **13**, **27**, **30**, **33**, and **36**, featuring substitution at the 4′-position, all showed high subtype selectivity for σ_1 over σ_2 receptors (37−187-fold) and, with the exception of the 4-propyl benzyl ether derivative **33**, high affinity for σ_1, with K_i values in the low nanomolar range (Table 1). The most potent compounds in this series were the 4′-methyl benzyl ether (**13**) and 4′-(2″-fluoroethyl) benzyl ether (**30**) derivatives, with σ_1 K_i values of 2.7 and 2.6 nM, respectively. Compound **30** displayed greater σ_1 selectivity (σ_2/σ_1 = 187, the greatest σ subtype selectivity within the series) than **13**, making it an ideal candidate as an ^{18}F-labeled radiotracer in PET imaging studies.

As compared to their 4′-substituted analogues, compounds **12**, **26**, **29**, **32**, and **35**, featuring substitution at the 3′-position, all showed substantially reduced σ_1 affinity but less pronounced attenuation of σ_2 affinity (Table 2). Consequently, all 3′-substituted analogues displayed moderate to poor levels of σ_1 versus σ_2 selectivity.

Compounds **11** and **28**, featuring substitution at the 2′-position, showed essentially no subtype selectivity, although the 2′-ethyl benzyl ether **25** and 2′-propyl benzyl ether **31** derivatives retained moderate affinity and modest selectivity for σ_1 receptors (Table 3). Compounds **11** and **28** did, however, display the highest affinity at the 5-HT_{2B} receptor (K_i = 9.7 and 57 nM, respectively), making them potential lead molecules for the development of selective 5-HT_{2B} drugs. The 2′-(3″-fluoropropyl) benzyl ether derivative **34** had a high affinity for σ_1 (K_i = 9.1 nM) and good subtype selectivity (σ_2/σ_1 = 60), a binding profile comparable to the 4′-substituted analogues within the series.

On the basis of these results, it is possible to make some tentative predictions regarding the requirements for σ_1 ligand binding and subtype selectivity. Alkyl ethers up to two carbon atoms long at the 4′-position appear to be well tolerated at the σ_1 binding site. The 4′-substituted derivatives containing a terminal fluorine atom show greater σ_1 affinity than their nonfluorinated counterparts, suggesting that an electrostatic interaction may be important. In general, substitution at either the 2′- or the 3′-position of the *N*-benzyl piperazine portion of molecule **10** led to poor subtype selectivity with the

Scheme 3. Synthesis of Ethyl-, (2″-Fluoroethyl)-, and Propyl Aryl Ether Derivatives **25**−**33**[a]

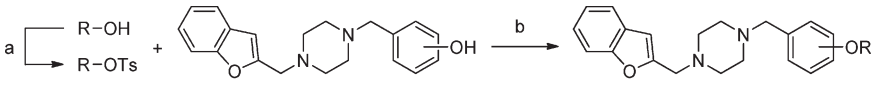

22 R = CH_2CH_3
23 R = CH_2CH_2F
24 R = $(CH_2)_2CH_3$

19-21

25 R = 2-OCH_2CH_3
26 R = 3-OCH_2CH_3
27 R = 4-OCH_2CH_3
28 R = 2-OCH_2CH_2F
29 R = 3-OCH_2CH_2F
30 R = 4-OCH_2CH_2F
31 R = 2-$OCH_2CH_2CH_3$
32 R = 3-$OCH_2CH_2CH_3$
33 R = 4-$OCH_2CH_2CH_3$

[a] Reagents and conditions: (a) TsCl, pyridine, CH_2Cl_2, 0 °C to RT, 3 h, 76−95%. (b) Appropriate phenol (**19**−**21**), K_2CO_3, DMF, reflux, 16 h, 60−73%.

Scheme 4. Synthesis of (3″-Fluoropropyl) Aryl Ether Derivatives **34**−**36**[a]

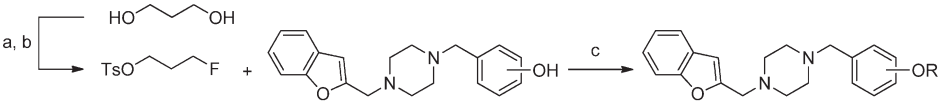

37

19-21

34 R = 2-$OCH_2CH_2CH_2F$
35 R = 3-$OCH_2CH_2CH_2F$
36 R = 4-$OCH_2CH_2CH_2F$

[a] Reagents and conditions: (a) TsCl (1.1 equiv), pyridine (1.1 equiv), CH_2Cl_2, 0 °C to RT, 4 h, 65%. (b) Deoxo-Fluor, CH_2Cl_2, RT, 24 h, 60%. (c) Appropriate phenol (**19**−**21**), K_2CO_3, DMF, reflux, 16 h, 61−63%.

Table 1. Affinities for 4′-Substituted *N*-Benzyl Piperazine Derivatives

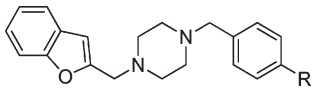

		$K_i \pm$ SEM (nM)[a]					
compd	R	5-HT_{1A}	5-HT_{2B}	D_2	σ_1	σ_2	σ_2/σ_1[b]
10	H	833 ± 130	497 ± 51	> 10000	5.2 ± 0.8	240 ± 47	46
13	OCH_3	2192 ± 395	15 ± 2	2700 ± 295	2.7 ± 0.4	103 ± 18	38
27	OCH_2CH_3	3339 ± 624	262 ± 37	4868 ± 982	10.6 ± 2.4	393 ± 93	37
30	OCH_2CH_2F	2439 ± 363	96 ± 13	> 10000	2.6 ± 0.6	486 ± 151	187
33	$O(CH_2)_2CH_3$	4722 ± 749	655 ± 66	> 10000	53.8 ± 7.7	2401 ± 669	45
36	$O(CH_2)_2CH_2F$	3300 ± 514	232 ± 23	> 10000	14.7 ± 2.1	752 ± 175	51

[a] Affinities were determined in rat brain homogenates using [^{3}H](+)-pentazocine for σ_1 and PC12 cells using [^{3}H]DTG for σ_2. The values in this table represent the means ± SEMs from triplicate assays. [b] This value is derived from the K_i for σ_2 binding affinity divided by the K_i for σ_1 binding affinity. Values > 1 indicate selectivity for σ_1 over σ_2.

Table 2. Affinities for 3′-Substituted *N*-Benzyl Piperazine Derivatives

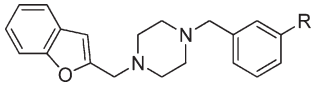

		$K_i \pm$ SEM (nM)[a]					
compd	R	5-HT_{1A}	5-HT_{2B}	D_2	σ_1	σ_2	σ_2/σ_1[b]
10	H	833 ± 130	497 ± 51	> 10000	5.2 ± 0.8	240 ± 47	46
12	OCH_3	373 ± 31	28 ± 3	5728 ± 905	16.3 ± 2.4	79.5 ± 11.4	4.9
26	OCH_2CH_3	1720 ± 258	302 ± 27	4542 ± 773	80 ± 13	238 ± 47	3.0
29	OCH_2CH_2F	469 ± 61	244 ± 25	2281 ± 387	49.7 ± 7.8	292 ± 67	5.9
32	$O(CH_2)_2CH_3$	774 ± 110	259 ± 28	2977 ± 425	177 ± 28	1919 ± 545	11
35	$O(CH_2)_2CH_2F$	599 ± 35	188 ± 20	2920 ± 259	232 ± 42	2371 ± 642	10

[a] Affinities were determined in rat brain homogenates using [^{3}H](+)-pentazocine for σ_1 and PC12 cells using [^{3}H]DTG for σ_2. The values in this table represent the means ± SEMs from triplicate assays. [b] This value is derived from the K_i for σ_2 binding affinity divided by the K_i for σ_1 binding affinity. Values > 1 indicate selectivity for σ_1 over σ_2.

notable exception of the 2′-(3″-fluoropropyl) benzyl ether derivative **34**. As compared to the lead compound **10**, the 4′-(2″-fluoroethyl) benzyl ether derivative **30** shows a 2-fold increase in σ_1 receptor affinity, a 4-fold increase in σ_1 versus σ_2 receptor selectivity, and a moderate affinity for the 5-HT_{2B} receptor subtype (K_i = 96 nM). Among the methyl benzyl

Table 3. Affinities for 2′-Substituted *N*-Benzyl Piperazine Derivatives

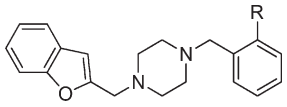

		$K_i \pm$ SEM (nM)[a]					
compd	R	5-HT_{1A}	5-HT_{2B}	D_2	σ_1	σ_2	σ_2/σ_1[b]
10	H	833 ± 130	497 ± 51	> 10000	5.2 ± 0.8	240 ± 47	46
11	OCH_3	806 ± 141	9.7 ± 1	5122 ± 1338	198 ± 29	89 ± 12	0.45
25	OCH_2CH_3	468 ± 50	72 ± 8	6005 ± 865	37.1 ± 7.8	295 ± 54	8.0
28	OCH_2CH_2F	3251 ± 605	57 ± 4	> 10000	488 ± 83	535 ± 101	1.1
31	$O(CH_2)_2CH_3$	2458 ± 215	116 ± 8	> 10000	79 ± 12	778 ± 134	10
34	$O(CH_2)_2CH_2F$	3383 ± 468	184 ± 20	> 10000	9.1 ± 1.6	542 ± 168	60

[a] Affinities were determined in rat brain homogenates using [^{3}H](+)-pentazocine for σ_1 and PC12 cells using [^{3}H]DTG for σ_2. The values in this table represent the means ± SEMs from triplicate assays. [b] This value is derived from the K_i for σ_2 binding affinity divided by the K_i for σ_1 binding affinity. Values > 1 indicate selectivity for σ_1 over σ_2.

Table 4. Summary of In Vitro σ_1 and σ_2 Binding Affinity and Lipophilicity Properties of **13**

K_i (nM)			
σ_1	σ_2	σ_2/σ_1	log *D*
2.7	103	38	3.63

ether analogues **11**−**13**, the 4′-methyl benzyl ether derivative **13** showed the greatest σ_1 affinity (K_i = 2.7 nM, comparable to **30**, a lead compound for fluorine-18 radiolabeling) and good subtype selectivity (σ_2/σ_1 = 38), indicating that it might be a suitable candidate for carbon-11 radiolabeling at the methyl ether position. This compound also showed high affinity for the 5-HT_{2B} receptor subtype (K_i = 15 nM). Prior to attempting the synthesis of [^{11}C]**13** for subsequent molecular imaging in a living system, it was necessary to examine the lipophilicity of **13**.

Lipophilicity Studies

Compounds having log *D* values >4.0 generally display a substantial nonspecific binding, reducing the target to nontarget ratios.[75] Using high-performance liquid chromatography (HPLC), a calibration curve correlating known log *D* values with the retention times of several reference compounds was obtained, and the log *D* value for piperazine **13** was determined from its average retention time over three runs.[76,77] Taking into consideration the in vitro binding data and the lipophilicity estimations (Table 4), ligand **13** appears to be a suitable candidate for the in vivo imaging of σ_1 receptors.

Radiochemistry and PET Studies

Phenol **21** was labeled with carbon-11 ($t_{1/2}$ = 20.4 min) to give [^{11}C]**13** in 22% nondecay corrected radiochemical yield, using [^{11}C]methyl iodide ([^{11}C]CH_3I) by standard *O*-alkylation (Scheme 5). [^{11}C]CH_3I was synthesized from cyclotron-produced [^{11}C]carbon dioxide ([^{11}C]CO_2), trapped in a *N*,*N*-dimethylformamide (DMF) solution containing **21** and tetra-*n*-butylammonium hydroxide (TBAH). This mixture was allowed to react at room temperature (RT) for 2 min, followed by heating at 80 °C for 5 min. The reaction mixture was purified by reverse phase semipreparative HPLC in an average synthesis time of 30 min (including HPLC purification and formulation). Coinjection of nonradioactive **13** was performed using analytical HPLC to confirm the identity of the product. In the final product solution, both radiochemical and chemical purities were greater than 98%, with a specific

Scheme 5. Synthesis of Radiolabeled Ligand [^{11}C]**13** from the Desmethyl Precursor **21**[a]

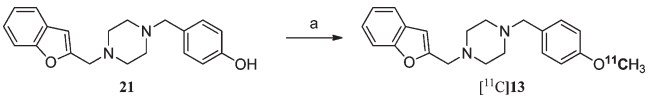

21 [^{11}C]**13**

[a] Reagents and conditions: (a) [^{11}C]CH_3I, TBAH, DMF, RT for 2 min, 80 °C for 5 min, followed by HPLC purification (XTerra C18).

activity of 73 GBq/μmol. No attempts were made to optimize these conditions, as sufficient quantities of the radioligand were produced to enable preliminary pharmacological evaluation. Formulation of radiolabeled product for intravenous injection was achieved following: (i) evaporation of the HPLC mobile phase, (ii) reconstitution of the residue in water for injections (5 mL), and (iii) sterile filtration through a 0.22 μm filter. The final injectable solution was clear and colorless, with a pH of 7.0. The preparation was free from labeling precursor **21**. Administration to the animal was performed within 10 min following the end of synthesis.

Evaluation Using PET

PET studies were conducted with an anaesthetized *Papio hamadryas* baboon to evaluate the in vivo regional distribution kinetics. Dynamic PET brain imaging commenced just prior to intravenous administration of [^{11}C]**13** (100 MBq in 3 mL of saline; specific activity 73 GBq/μmol) and was terminated 60 min postinjection. This was immediately followed by a whole body acquisition for 2 min at each of the six bed positions. The PET images confirmed the ability of [^{11}C]**13** to traverse the blood−brain barrier with considerable accumulation of radioactivity in the baboon brain (Figure 3). Second, the in vivo specificity and selectivity of [^{11}C]**13** in the baboon brain were assessed 3 weeks after initial PET evaluation via a blocking study using **1** (1 mg/kg, iv).

Time−activity curves for the uptake of [^{11}C]**13** in the baboon brain (Figure 4) showed homogeneous uptake of [^{11}C]**13** in the cingulate cortex, frontal cortex, striatum, thalamus, and cerebellum, which are responsible for motor function and known to contain σ-receptors.[78,79] Brain uptake of [^{11}C]**13** reached maximal levels 5 min postinjection and remained at a plateau to the end of the scan. Whole body images of the baboon (Figure 6A), acquired at the conclusion of dynamic screening, clearly show uptake of [^{11}C]**13** by the brain, as well as organs outside the CNS. In particular, there

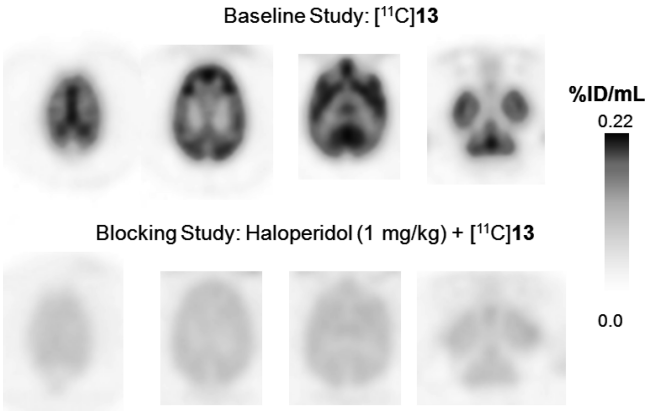

Figure 3. *P. hamadryas* baboon PET summation images of selected transaxial brain slices over 60 min.

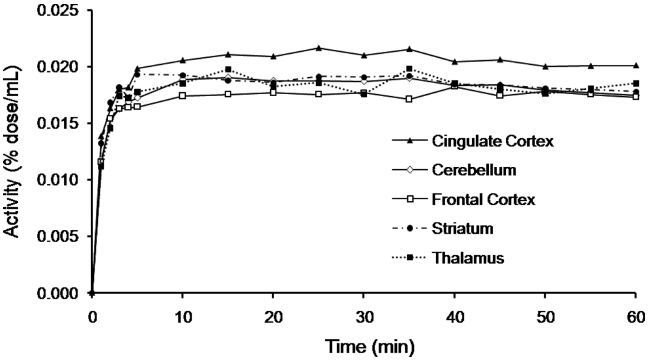

Figure 4. Time−activity curves depicting uptake of [^{11}C]**13** in selected regions of the *P. hamadryas* baboon brain during a 60 min PET scan.

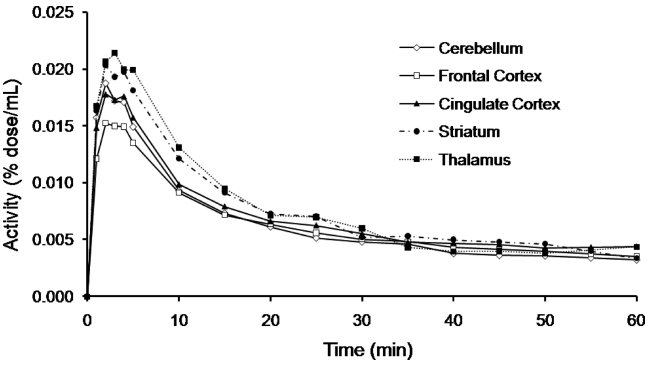

Figure 5. Time−activity curves depicting uptake of [^{11}C]**13** pretreated with **1** in selected regions of the *P. hamadryas* baboon brain during a 60 min PET scan.

was substantial uptake of [^{11}C]**13** by the liver, which is known to contain a high density of σ_1 receptors.

Pretreatment of the baboon with **1** 5 min prior to [^{11}C]**13** injection resulted in an initial increase in [^{11}C]**13** uptake 3 min postinjection, followed by washout. There was a reduced uptake of 80% of the radioligand in all regions of the brain, which was maintained to the end of the scan (Figure 5). Similar results have been reported for other **1** blocking studies.[80−83] Figure 6B shows the whole body images of the baboon, which were acquired at the conclusion of dynamic screening. These images demonstrate significant inhibition of [^{11}C]**13** uptake in the brain and liver, as well as accumulation

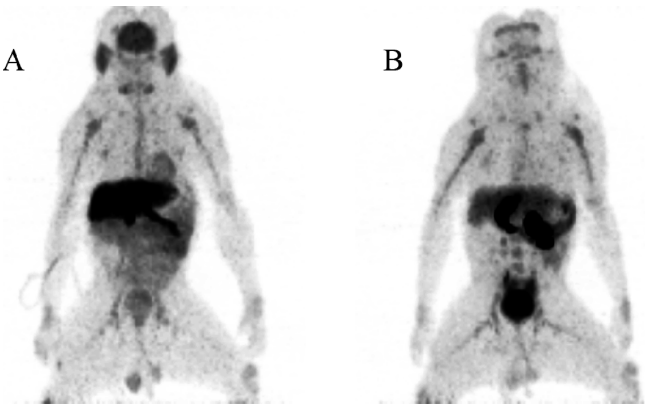

Figure 6. PET images of whole *P. hamadryas* baboon brain during 60 min after intravenous injection of [^{11}C] (baseline; A) and [^{11}C]**13** plus **1** (1 mg/kg; B).

of [^{11}C]**13** in the kidneys and bladder, indicative of metabolism and excretion of the radioligand. Complete displacement of [^{11}C]**13** binding in the aforementioned CNS and PNS regions demonstrates the ease of displacing [^{11}C]**13** and denotes specific σ_1 binding outside the brain.

Conclusion

We have developed a series of potent and subtype selective σ receptor ligands, based on lead structure **10**. Exploration of benzylic substitution of **10** led us to synthesize regioisomeric benzylic piperazines bearing alkyl and fluoroalkyl aryl ethers (**11**−**13** and **25**−**36**). The σ receptor affinities of these regioisomers revealed that aryl ethers at the 4′-position are generally well tolerated at σ_1, with comparable subtype selectivity to that of **10**. In the case of 4′-substituted aryl alkyl ethers, a terminal fluorine atom on the alkyl chain enhances both σ_1 affinity and σ_1 subtype selectivity, as compared to the respective nonfluorinated analogues. Within this series, the 4′-(2″-fluoroethoxy) derivative **30** was identified as a high-affinity σ_1 receptor ligand (K_i = 2.6 nM), with good subtype selectivity (σ_2/σ_1 = 187), and negligible affinity for other CNS receptors except the 5-HT$_{2B}$ receptor for which it shows moderate affinity (K_i = 96 nM).

The 4′-methoxy analogue from this class (**13**), also a highly selective σ_1 ligand, was identified as a candidate for carbon 11 radiolabeling to produce a σ_1 receptor PET imaging agent. Preparation of [^{11}C]**13** was achieved in good radiochemical yield, and this compound was shown to cross the blood−brain barrier and bind to σ_1 receptors in baboon brain and peripheral organs in vivo. The pharmacological profile of [^{11}C]**13** makes it a useful probe for evaluating the roles of σ_1 receptors in neurodegenerative processes in vivo.

In conclusion, we have developed a series of *N*-benzyl alkyl ether piperazine derivatives as high affinity and subtype selective σ_1 receptor ligands, which warrant further investigation into their potential therapeutic applications for the treatment of CNS disorders. This class of compounds can also serve as diagnostic probes when radiolabeled to not only elucidate the role of σ receptors in the onset and progression of disease but also to monitor the efficacy of therapeutic regimes.

Experimental Section

Chemistry. Melting point determinations were carried out on an Optimelt Automated Melting Point System and are recorded uncorrected. ^{1}H NMR spectra were acquired at 300 K using a

Bruker Avance DP X300 (300 MHz) as solutions in D_2O or $CDCl_3$, where residual H_2O (δ 4.79 ppm) and $CHCl_3$ (δ 7.26 ppm) were used as respective internal references. Data are reported as chemical shifts (δ ppm), relative integral, multiplicity (s = singlet, br s = broad singlet, d = doublet, dd = doublet of doublets, dt = double of triplets, t = triplet, m = multiplet, and dm = doublet of multiplets), and coupling constants (J, Hz). Solvent peaks for chloroform (δ 77.16) were used as the internal reference for ^{13}C NMR spectra. Residual acid in deuterated chloroform was removed prior to use by filtering through a pad of basic alumina. Low-resolution mass spectra were recorded on a Finnigan LCQ mass spectrometer. High-resolution mass spectra were recorded by the Mass Spectrometry Unit of the School of Chemistry, University of New South Wales. Positive electrospray ionization (+ESI) utilized methanol and/or dichloromethane. The purity of all new compounds was ≥95% based on C, H, and N analyses, conducted at the Campbell Microanalytical Laboratory, Chemistry Department at University of Otago, New Zealand. Analytical thin layer chromatography was carried out using aluminum-backed silica gel 60 F_{254} Merck KGaA sheets, and plates were visualized under a UV lamp at λ = 254 nm. Flash chromatography employed Merck Kieselgel 60 (230−400 mesh) silica gel. Solvents for flash column chromatography were distilled prior to use. Tetrahydrofuran was dried over sodium wire and distilled from benzophenone. Dichloromethane was distilled from calcium hydride. DMF was distilled from calcium hydride and stored over activated 4 Å molecular sieves. Piperazine was recrystallized from absolute ethanol. Anhydrous K_2CO_3 was ground and dried at 140 °C in the oven for at least 2 days prior to use. 4-Hydroxybenzaldehyde was recrystallized from distilled water. 1,2-Dichloroethane was distilled from and stored over calcium hydride. Ethanol, *n*-propanol, and pyridine were distilled from calcium hydride and stored over activated 3 Å molecular sieves. Crude tosyl chloride (~10 g) was dissolved in chloroform (25 mL), filtered, and diluted with hexanes (125 mL) to precipitate impurities. The solution was then filtered, clarified with charcoal, and concentrated under reduced pressure to give analytically pure material (~7 g). 2-Fluoroethanol was purchased from Matrix Scientific and used without further purification. Remaining reagents were purchased from Sigma Aldrich Chemical Co. and used without further purification.

***tert*-Butyl Piperazine-1-carboxylate (15).**[71−73] To a solution of 1,4-piperazine (3.44 g, 39.9 mmol, 2.0 equiv) in CH_2Cl_2 (100 mL) at RT was added a solution of Boc_2O (4.6 mL, 20 mmol, 1.0 equiv) in CH_2Cl_2 (50 mL) over a period of 3 h after which the reaction mixture was stirred at RT for 22 h. The solvent was evaporated, and the residue thus obtained was treated with H_2O (100 mL). The precipitated product was collected by filtration, and the filtrate was further extracted with CH_2Cl_2 (3 × 100 mL). The combined organic fractions were dried (Na_2SO_4) and concentrated in vacuo to give the title compound as a colorless solid (3.01 g combined yield, 81%); mp 46−47 °C (lit. mp 46−47 °C).[71−73] ^1H NMR (300 MHz, $CDCl_3$): δ 1.46 (9H, s), 2.42 (1H, s), 2.82 (4H, t, J = 5.1 Hz), 3.40 (4H, t, J = 5.2 Hz). The spectroscopic data matched that reported in the literature.[71−73]

***tert*-Butyl 4-(Benzofuran-2-carbonyl)piperazine-1-carboxylate (16).** To a suspension of 1-ethyl-3-(3-dimethylaminopropyl)-carbodiimide hydrochloride (EDC·HCl) (5.68 g, 29.6 mmol, 1.20 equiv) and *N*-methylmorpholine (NMM) (10.8 mL, 98.8 mmol, 4.00 equiv) in DMF (160 mL) were added successively *N*-hydroxybenzotriazole (HOBt) (4.00 g, 29.6 mmol, 1.20 equiv), benzofuran-2-carboxylic acid (4.00 g, 24.7 mmol, 1.00 equiv), and **15** (4.60 g, 24.7 mmol). The reaction mixture was stirred at RT for 20 h and then diluted with H_2O (400 mL) and extracted with EtOAc (3 × 400 mL). The combined organic fractions were washed with brine, dried (Na_2SO_4), and concentrated under reduced pressure. Purification of the crude residue by flash chromatography on silica gel (hexanes:EtOAc, 80:20 → 75:25 → 70:30) afforded the title compound as a colorless solid (6.82 g, 84%); mp 97−98 °C; R_f 0.19 (hexanes:EtOAc, 70:30). ^1H NMR (300 MHz, $CDCl_3$): δ 1.49 (9H, s), 3.55 (4H, t, J = 8.6 Hz), 3.84 (4H, br s), 7.30 (1H, dd, J = 7.5, 7.5 Hz), 7.35 (1H, s), 7.41 (1H, dd, J = 7.6, 7.8 Hz), 7.53 (1H, d, J = 8.3 Hz), 7.66 (1H, d, J = 7.7 Hz). ^{13}C NMR (75.5 MHz, $CDCl_3$): δ 28.8, 30.1, 44.1, 80.8, 112.3, 112.9, 122.7, 124.1, 127.1, 127.3, 149.2, 155.0, 155.1, 160.3. HRMS (+ESI) calcd for $C_{18}H_{22}N_2O_4$ m/z: $[M + Na]^+$, 353.1472; found, 353.1464.

Benzofuran-2-yl(piperazin-1-yl)methanone Hydrochloride (17). *tert*-Butyl 4-(benzofuran-2-carbonyl)piperazine-1-carboxylate (**16**) (6.82 g, 20.7 mmol) was added to a solution of HCl in dioxane (4 M, 20 mL) and stirred at RT for 30 min. The reaction mixture was concentrated in vacuo to give the title compound as a colorless solid (5.52 g, quantitative); mp 234−235 °C. ^1H NMR (300 MHz, D_2O): δ 3.42 (4H, t, J = 5.1 Hz), 4.11 (4H, br s), 7.40 (1H, dd, J = 7.3, 7.6 Hz), 7.45 (1H, s), 7.54 (1H, dd, J = 7.2, 8.2 Hz), 7.62 (1H, d, J = 8.3 Hz), 7.78 (1H, d, J = 7.8 Hz). ^{13}C NMR (75.5 MHz, D_2O): δ 40.5, 43.5, 112.2, 114.1, 123.2, 124.4, 126.8, 128.0, 146.6, 155.0, 161.7. HRMS (+ESI) calcd for $C_{13}H_{14}N_2O_2$ m/z: $[M + H]^+$, 231.1128; found, 231.1128.

***N*-((Benzofuran-2-yl)methyl)piperazine (18).** To a suspension of $LiAlH_4$ (2.36 g, 66.9 mmol, 3.25 equiv) in anhydrous THF (216 mL) at 0 °C was added, portionwise, $AlCl_3$ (2.76 g, 20.6 mmol, 1.00 equiv). Stirring was continued at 0 °C for 15 min prior to the portionwise addition of free base of **17** (4.77 g, 20.6 mmol, 1.00 equiv). The reaction mixture was stirred at 0 °C for 2 h after which time it was quenched by the successive addition of H_2O (2.4 mL), aqueous NaOH (4 M, 2.4 mL), and H_2O (7.2 mL). The resultant mixture was filtered, the filtrate was partitioned with CH_2Cl_2 (300 mL), and the aqueous phase was isolated and further extracted with CH_2Cl_2 (2 × 300 mL). The combined organic fractions were washed with brine, dried (Na_2SO_4), and concentrated under reduced pressure. Purification of the crude residue by flash chromatography on silica gel (CH_2Cl_2:MeOH: aqueous NH_4OH, 90:10:0.1) afforded the title compound as a pale yellow solid (3.36 g, 75%); mp 173−174 °C; R_f 0.20 (CH_2Cl_2:MeOH:aqueous NH_4OH, 90:10:0.1). ^1H NMR (300 MHz, $CDCl_3$): δ 2.11 (1H, br s), 2.51 (4H, br s), 2.92 (4H, t, J = 9.6 Hz), 3.66 (2H, s), 6.58 (1H, s), 7.16−7.26 (2H, m), 7.45−7.52 (2H, m). ^{13}C NMR (75.5 MHz, $CDCl_3$): δ 45.9, 54.3, 56.0, 105.8, 111.3, 120.7, 122.7, 123.9, 128.3, 154.4, 155.1. HRMS (+ESI) calcd for $C_{13}H_{16}N_2O$ m/z: $[M + H]^+$, 217.1335; found, 217.1331.

General Procedure for *N*-Alkylation. To a suspension of *N*-((benzofuran-2-yl)methyl)piperazine **18** (216 mg, 1.00 mmol) and anhydrous K_2CO_3 (552 mg, 4.00 mmol) in DMF (5 mL) at RT were added NaI (15 mg, 0.1 mmol) and the appropriate benzyl alkyl halide (1.1 equiv). The reaction mixture was heated at reflux for 20 h before cooling to ambient temperature. H_2O (100 mL) was added, and the mixture was extracted with EtOAc (3 × 60 mL). The combined organic fractions were washed with brine, dried (Na_2SO_4), and concentrated under reduced pressure to give a crude residue, which was purified by flash chromatography on silica gel (CH_2Cl_2:MeOH, 99:1).

***N*-((Benzofuran-2-yl)methyl)-*N*′-benzylpiperazine (10).** Treatment of **18** with benzyl bromide according to the method described above afforded the title compound as a pale yellow oil (251 mg, 82%); R_f 0.42 (CH_2Cl_2:MeOH, 99:1). ^1H NMR (300 MHz, $CDCl_3$): δ 2.54 (8H, br s), 3.51 (2H, s), 3.69 (2H, s), 6.58 (1H, s), 7.16−7.37 (7H, m), 7.48 (2H, d, J = 7.9 Hz). ^{13}C NMR (75.5 MHz, $CDCl_3$): δ 53.0, 53.2, 55.6, 63.1, 105.8, 111.4, 120.8, 122.8, 124.7, 127.2, 127.5, 128.3, 129.4, 139.0, 154.2, 154.6. HRMS (+ESI) calcd for $C_{20}H_{22}N_2O$ m/z: $[M + H]^+$, 307.1805; found, 306.1753.

***N*-((Benzofuran-2-yl)methyl)-*N*′-(2′-methoxybenzyl)piperazine (11).** Treatment of **18** with 2-methoxybenzyl chloride according to the method described above afforded the title compound as a dark yellow oil (270 mg, 81%); R_f 0.39 (CH_2Cl_2:MeOH, 99:1). ^1H NMR (300 MHz, $CDCl_3$): δ 2.60 (8H, br s), 3.61 (2H, s), 3.69 (2H, s), 3.80 (3H, s), 6.58 (1H, s), 6.86 (1H, dd, J = 6.9, 8.2 Hz),

6.92 (1H, d, J = 7.4 Hz), 7.16−7.26 (3H, m), 7.32 (1H, d, J = 7.4 Hz), 7.49 (2H, dd, J = 5.9, 8.8 Hz). ^{13}C NMR (75.5 MHz, $CDCl_3$): δ 52.8, 53.2, 55.6, 56.0, 56.2, 105.8, 110.6, 111.4, 120.4, 120.8, 121.9, 122.7, 124.0, 128.3, 128.6, 130.8, 153.7, 154.5, 162.5. HRMS (+ESI) calcd for $C_{21}H_{24}N_2O_2$ m/z: $[M + H]^+$, 337.1911; found, 337.1909.

***N*-((Benzofuran-2-yl)methyl)-*N*′-(3′-methoxybenzyl)piperazine (12).** Treatment of **18** with 3-methoxybenzyl bromide according to the method described above afforded the title compound as a pale yellow solid (279 mg, 83%); mp 83−84 °C; R_f 0.35 (CH_2Cl_2:MeOH, 99:1). ^{1}H NMR (300 MHz, $CDCl_3$): δ 2.48 (8H, br s), 3.41 (2H, s), 3.62 (2H, s), 3.73 (3H, s), 6.58 (1H, s), 6.77−6.80 (1H, m), 6.87−6.90 (2H, m), 7.17−7.26 (3H, m), 7.45−7.53 (2H, m). ^{13}C NMR (75.5 MHz, $CDCl_3$): δ 53.4, 53.6, 55.8, 56.0, 63.4, 105.7, 111.9, 113.1, 115.2, 121.2, 122.1, 123.1, 124.4, 128.9, 129.7, 140.3, 155.1, 155.7, 160.2. HRMS (+ESI) calcd for $C_{21}H_{24}N_2O_2$ m/z: $[M + H]^+$, 337.1911; found, 337.1913.

***N*-((Benzofuran-2-yl)methyl)-*N*′-(4′-methoxybenzyl)piperazine (13).** Treatment of **18** with 4-methoxybenzyl chloride according to the method described above afforded the title compound as a pale yellow solid (282 mg, 84%); mp 93−94 °C; R_f 0.17 (CH_2Cl_2:MeOH, 99:1). ^{1}H NMR (300 MHz, $CDCl_3$): δ 2.55 (8H, br s), 3.48 (2H, s), 3.70 (2H, s), 3.79 (3H, s), 6.58 (1H, s), 6.81−6.86 (2H, m), 7.18−7.27 (4H, m), 7.44−7.53 (2H, m). ^{13}C NMR (75.5 MHz, $CDCl_3$): δ 52.6, 52.9, 55.2, 55.4 (CH_2), 62.2 (CH_2), 105.7 (CH), 111.3 (CH), 113.6 (CH), 120.7 (CH), 122.6 (CH), 123.9 (CH, C), 128.3 (C), 130.5 (CH), 154.4 (C), 155.1 (C), 158.8 (C). HRMS (+ESI) calcd for $C_{21}H_{24}N_2O_2$ m/z: $[M + H]^+$, 337.1911; found, 337.1910.

General Procedure for Phenol Synthesis. The appropriately substituted hydroxybenzaldehyde (1.1 equiv) was added to a solution of *N*-((benzofuran-2-yl)methyl)piperazine **18** (3.07 g, 14.2 mmol) in DCE (71 mL) at RT, and stirring was continued for 15 min prior to the portionwise addition of $NaBH(OAc)_3$ (3.48 g, 22.7 mmol, 1.60 equiv). The reaction mixture was stirred at RT for 4 h after which time it was quenched with saturated aqueous $NaHCO_3$ (150 mL). The aqueous phase was extracted with CH_2Cl_2 (3 × 200 mL), and the combined organic extracts were washed with brine, dried (Na_2SO_4), and concentrated under reduced pressure to give the crude product, which was purified by flash chromatography on silica gel.

***N*-((Benzofuran-2-yl)methyl)-*N*′-(2′-hydroxybenzyl)piperazine (19).** Treatment of **18** with 2-hydroxybenzaldehyde according to the method described above afforded the title compound as a dark yellow solid (3.80 g, 83%); mp 126−127 °C; R_f 0.39 (hexanes:EtOAc, 75:25). ^{1}H NMR (300 MHz, $CDCl_3$): δ 2.64 (8H, br s), 3.71 (4H, s), 4.88 (1H, s), 6.60 (1H, s), 6.75−6.91 (2H, m), 6.97 (1H, d, J = 7.3 Hz), 7.17−7.28 (3H, m), 7.47 (1H, d, J = 7.7 Hz), 7.53 (1H, d, J = 7.3 Hz). ^{13}C NMR (75.5 MHz, $CDCl_3$): δ 52.9, 53.4, 55.8, 61.9, 106.5, 111.9, 116.6, 117.1, 121.3, 121.7, 123.3, 124.6, 128.8, 129.2, 154.6, 155.7, 158.3. MS (+ESI) m/z: 323.27 ($[M + H]^+$, 100%). Anal. ($C_{20}H_{22}N_2O_2$) calcd: C, 74.51; H, 6.88; N, 8.69. Found: C, 74.39; H, 6.71; N, 8.71.

***N*-((Benzofuran-2-yl)methyl)-*N*′-(3′-hydroxybenzyl)piperazine (20).** Treatment of **18** with 3-hydroxybenzaldehyde according to the method described above afforded the title compound as a colorless solid (3.85 g, 84%); mp 124−125 °C; R_f 0.36 (CH_2Cl_2:MeOH, 95:5). ^{1}H NMR (300 MHz, $CDCl_3$): δ 2.54 (8H, br s), 3.44 (2H, s), 3.68 (2H, s), 4.60 (1H, s), 6.56 (1H, s), 6.65−6.72 (2H, m), 6.79 (1H, d, J = 7.6 Hz), 7.09−7.16 (1H, m), 7.18−7.23 (2H, m), 7.42 (1H, d, J = 7.9 Hz), 7.50 (1H, d, J = 6.7 Hz). ^{13}C NMR (75.5 MHz, $CDCl_3$): δ 53.2, 53.8, 63.3, 106.5, 111.9, 115.0, 117.0, 121.3, 122.0, 123.2, 124.5, 128.2, 128.8, 130.1, 139.5, 154.6, 155.6, 156.6. MS (+ESI) m/z: 323.13 ($[M + H]^+$, 100%). Anal. ($C_{20}H_{22}N_2O_2$) calcd: C, 74.51; H, 6.88; N, 8.69. Found: C, 74.31; H, 6.81; N, 8.79.

***N*-((Benzofuran-2-yl)methyl)-*N*′-(4′-hydroxybenzyl)piperazine (21).** Treatment of **18** with 4-hydroxybenzaldehyde according to the method described above afforded the title compound as a colorless solid (3.89 g, 85%); mp 148−149 °C; R_f 0.33 (CH_2Cl_2:MeOH, 95:5). ^{1}H NMR (300 MHz, $CDCl_3$): δ 2.59 (8H, br s), 3.46 (2H, s), 3.68 (2H, s), 6.57 (2H, br s), 6.60 (1H, s), 7.05 (2H, d, J = 8.4 Hz), 7.15−7.25 (2H, m), 7.41 (1H, d, J = 8.0 Hz), 7.49 (1H, d, J = 7.0 Hz). ^{13}C NMR (75.5 MHz, $CDCl_3$): δ 52.8, 53.2, 55.8, 62.8, 106.5, 111.9, 116.1, 121.3, 123.2, 124.6, 128.2, 128.8, 131.6, 154.5, 155.6, 156.2. HRMS (+ESI) calcd for $C_{20}H_{22}N_2O_2$ m/z: $[M + H]^+$, 323.1754; found, 323.1765.

General Procedure for Tosylate Synthesis.[84] To a solution of the alcohol (4 mmol, 1 equiv) in CH_2Cl_2 (4 mL) at 0 °C were added tosyl chloride (0.84 g, 4.4 mmol, 1.1 equiv) and pyridine (0.36 mL, 4.4 mmol, 1.1 equiv). The reaction mixture was warmed to RT and stirred for 3 h. H_2O (20 mL) and saturated aqueous NH_4Cl (10 mL) were added, and the mixture was extracted with CH_2Cl_2 (3 × 60 mL). The combined organic fractions were washed with brine, dried (Na_2SO_4), and concentrated under reduced pressure to give the crude product, which was purified by flash chromatography on silica gel (hexanes:CH_2Cl_2, 50:50).

Ethyl Tosylate (22). The treatment of ethanol with tosyl chloride according to the method described above afforded the title compound as a colorless oil (0.62 g, 78%); R_f 0.41 (hexanes:CH_2Cl_2, 50:50). ^{1}H NMR (300 MHz, $CDCl_3$): δ 1.28 (3H, t, J = 7.2 Hz), 2.44 (3H, s), 4.11 (2H, q, J = 7.1 Hz) 7.35 (2H, d, J = 8.2 Hz), 7.80 (2H, d, J = 8.3 Hz). ^{13}C NMR (75.5 MHz, $CDCl_3$): δ 14.4, 21.3, 66.5, 127.6, 129.5, 133.0, 144.4. HRMS (+ESI) calcd for $C_9H_{12}O_3S$ m/z: $[M + Na]^+$, 223.0399; found, 223.0400.

2-Fluoroethyl Tosylate (23). The treatment of 2-fluoroethanol with tosyl chloride according to the method described above afforded the title compound as a colorless oil (0.74 g, 85%); R_f 0.34 (hexanes:CH_2Cl_2, 50:50). ^{1}H NMR (400 MHz, $CDCl_3$): δ 2.45 (3H, s, CH_3), 4.21−4.30 (2H, dm, J = 27 Hz), 4.49−4.63 (2H, dm, J = 47 Hz), 7.35 (2H, d, J = 8.0 Hz), 7.80 (2H, d, J = 7.5 Hz). The spectroscopic data matched those reported in the literature.[85]

***n*-Propyl Tosylate (24).** The treatment of *n*-propanol with tosyl chloride according to the method described above afforded the title compound as a colorless oil (0.75 g, 88%); R_f 0.34 (hexanes:CH_2Cl_2, 50:50). ^{1}H NMR (300 MHz, $CDCl_3$): δ 0.90 (3H, t, J = 7.4 Hz), 1.63−1.73 (2H, m), 2.45 (3H, s), 3.99 (2H, dd, J = 6.5, 6.5 Hz), 7.35 (2H, d, J = 8.0 Hz), 7.79 (2H, d, J = 8.1 Hz). ^{13}C NMR (75.5 MHz, $CDCl_3$): δ 10.5, 22.1, 22.8, 72.7, 128.4, 130.2, 133.8, 145.2. HRMS (+ESI) calcd for $C_{10}H_{14}O_3S$ m/z: $[M + Na]^+$, 237.0556; found, 237.0556.

3-Fluoropropyl Tosylate (37). To a solution of 1,3-propanediol (0.30 mL, 4.0 mmol, 1.0 equiv) in CH_2Cl_2 (4 mL) at 0 °C were added tosyl chloride (0.84 g, 4.4 mmol, 1.1 equiv) portionwise and pyridine (0.36 mL, 4.4 mmol, 1.1 equiv) dropwise. The reaction mixture was warmed to RT and stirred for 4 h. H_2O (20 mL) and saturated aqueous NH_4Cl (10 mL) were added, and the mixture was extracted with CH_2Cl_2 (3 × 60 mL). The combined organic fractions were washed with brine, dried (Na_2SO_4), and concentrated in vacuo. Purification of the crude material thus obtained by flash chromatography on silica gel (hexanes:EtOAc, 50:50) afforded 3-hydroxypropyl 4-methylbenzensulfonate as a colorless oil (0.60 g, 65%); R_f 0.33 (hexanes:EtOAc, 50:50). ^{1}H NMR ($CDCl_3$, 300 MHz): δ 1.82−1.90 (2H, m), 2.44 (3H, s), 2.63 (1H, s), 3.65 (2H, t, J = 6.0 Hz), 4.07 (2H, t, J = 6.2 Hz), 7.35 (2H, d, J = 8.3 Hz), 7.75 (2H, d, J = 8.3 Hz). ^{13}C NMR ($CDCl_3$, 75.5 MHz): δ 22.0, 32.0, 58.5, 68.1, 128.0, 130.5, 133.1, 145.4. HRMS (+ ESI) calcd for $C_{10}H_{14}O_4S$ m/z: $[M + Na]^+$, 253.0505; found, 253.0511.

To a solution of 3-hydroxypropyl 4-methylbenzensulfonate (0.60 g, 2.6 mmol, 1.0 equiv) in CH_2Cl_2 (8 mL) at RT was added bis(2-methoxyethyl)aminosulfur trifluoride (Deoxo Fluor, 0.52 mL, 2.86 mmol, 1.1 equiv). The reaction mixture was stirred at RT for 24 h after which time saturated aqueous $NaHCO_3$ was added dropwise until the pH reached 8. The mixture was extracted with CH_2Cl_2 (3 × 60 mL), washed with brine, dried (Na_2SO_4), and concentrated in vacuo. Purification of the crude

residue thus obtained by flash chromatography on silica gel (hexanes:EtOAc, 50:50) afforded the title compound as a pale yellow oil (0.56 g, 60%); R_f 0.78 (hexanes:EtOAc, 50:50). ^{1}H NMR ($CDCl_3$, 400 MHz): δ 1.99−2.09 (2H, m), 2.45 (3H, s), 4.16 (2H, t, J = 6.2 Hz), 4.41−4.45 (2H, dt, J = 47 Hz), 7.36 (2H, d, J = 8.0 Hz), 7.80 (2H, d, J = 8.0 Hz). ^{13}C NMR ($CDCl_3$, 75.5 MHz): δ 22.2, 30.6, 66.6, 79.0, 81.2, 128.4, 130.6, 133.4, 145.5. HRMS (+ ESI) calcd for $C_{10}H_{13}FO_3S$ m/z: $[M + Na]^+$, 255.0462; found, 255.0463.

General Procedure for *O*-Alkylation. To a suspension of the appropriately substituted phenol (322 mg, 1.00 mmol) and K_2CO_3 (522 mg, 4.00 mmol) in DMF (2.5 mL) at RT was added a solution of the appropriate tosylate (2.00 mmol) in DMF (2.5 mL). The reaction mixture was heated at reflux for 15 h, cooled to RT, treated with H_2O (100 mL), and extracted with EtOAc (3 × 60 mL). The combined organic fractions were washed with brine, dried (Na_2SO_4), and concentrated under reduced pressure to give the crude product, which was purified by flash chromatography on silica gel.

***N*-((Benzofuran-2-yl)methyl)-*N*′-(2′-ethoxybenzyl)piperazine (25).** The treatment of phenol **19** with ethyl tosylate (**22**) according to the method described above afforded the title compound as a yellow oil (217 mg, 62%); R_f 0.34 (hexanes:EtOAc, 80:20). ^{1}H NMR (300 MHz, $CDCl_3$): δ 1.39 (3H, t, J = 6.9 Hz), 2.59 (8H, br s), 3.62 (2H, s), 3.70 (2H, s), 4.03 (2H, q, J = 6.9 Hz), 6.59 (1H, s), 6.75−6.98 (2H, m), 7.14−7.33 (4H, m), 7.45−7.54 (2H, m). ^{13}C NMR (75.5 MHz, $CDCl_3$): δ 15.3, 52.7, 53.0, 55.7, 56.2, 64.5, 106.0, 111.7, 120.0, 120.6, 121.0, 123.0, 124.2, 126.0, 127.9, 128.4, 129.2, 154.3, 154.8, 159.0. HRMS (+ESI) calcd for $C_{22}H_{26}N_2O_2$ m/z: $[M + H]^+$, 351.2067; found, 351.2069.

***N*-(Benzofuran-2-ylmethyl)-*N*′-(3′-ethoxybenzyl)piperazine (26).** The treatment of phenol **20** with ethyl tosylate (**22**) according to the method described above afforded the title compound as a golden oil (232 mg, 66%); R_f 0.29 (hexanes:EtOAc, 70:30). ^{1}H NMR (300 MHz, $CDCl_3$): δ 1.39 (3H, t, J = 7.0 Hz), 2.55 (8H, br s), 3.48 (2H, s), 3.69 (2H, s), 4.02 (2H, q, J = 7.0 Hz), 6.58 (1H, s), 6.77 (1H, d, J = 5.9 Hz), 6.86−6.88 (2H, m), 7.16−7.26 (3H, m), 7.49 (2H, dd, J = 7.1,7.7 Hz). ^{13}C NMR (75.5 MHz, $CDCl_3$): δ 15.4, 53.4, 53.6, 56.0, 63.5, 63.9, 106.2, 111.9, 113.6, 115.8, 121.2, 121.9, 123.2, 124.4, 127.5, 129.7, 140.3, 155.1, 159.5. HRMS (+ESI) calcd for $C_{22}H_{26}N_2O_2$ m/z: $[M + H]^+$, 351.2067; found, 351.2066.

***N*-(Benzofuran-2-ylmethyl)-*N*′-(4′-ethoxybenzyl)piperazine (27).** The treatment of phenol **21** with ethyl tosylate (**22**) according to the method described above afforded the title compound as a yellow solid (231 mg, 66%); mp 63−64 °C; R_f 0.28 (hexanes:EtOAc, 50:50). ^{1}H NMR (300 MHz, $CDCl_3$): δ 1.36 (3H, t, J = 7.0 Hz), 2.54 (8H, br s), 3.44 (2H, s), 3.69 (2H, s), 4.04 (2H, q, J = 7.0 Hz), 6.58 (1H, s), 6.82 (2H, d, J = 8.4 Hz), 7.18−7.24 (4H, m), 7.69 (2H, d, J = 7.3 Hz). ^{13}C NMR (75.5 MHz, $CDCl_3$): δ 15.0, 52.9, 53.1, 55.5, 62.5, 63.6, 105.8, 111.4, 114.3, 120.8, 122.8, 124.0, 127.9, 130.6, 132.2, 154.6, 158.3. MS (+ESI) m/z: 351.27 ($[M + H]^+$, 100%). Anal. ($C_{22}H_{26}N_2O_2$) calcd: C, 75.40; H, 7.48; N, 7.99. Found: C, 75.25; H, 7.49; N, 8.05.

***N*-((Benzofuran-2-yl)methyl)-*N*′-(2′-(2″-fluoroethoxy)benzyl)-piperazine (28).** The treatment of phenol **19** with 2-fluoroethyl tosylate (**23**) according to the method described above afforded the title compound as a pale yellow oil (269 mg, 73%); R_f 0.29 (hexanes:EtOAc, 60:40). ^{1}H NMR (300 MHz, $CDCl_3$): δ 2.59 (8H, br s), 3.64 (2H, s), 3.68 (2H, s), 4.13−4.25 (2H, dt, J = 4.1 Hz, J = 28 Hz,), 4.63−4.82 (2H, dt, J = 4.3 Hz, J = 47 Hz), 6.57 (1H, s), 6.83 (1H, d, J = 8.2 Hz), 6.94 (1H, dd, J = 7.4, 7.4 Hz), 7.15−7.25 (3H, m), 7.33 (1H, d, J = 7.4 Hz), 7.48 (2H, d, J = 7.5 Hz). ^{13}C NMR (75.5 MHz, $CDCl_3$): δ 52.7, 53.2, 55.6, 55.9, 67.7, 67.9, 105.8, 111.5, 112.1, 120.8, 121.2, 122.7, 124.0, 126.1, 127.9, 128.3, 131.3, 154.2, 154.9, 159.0. HRMS (+ESI) calcd for $C_{22}H_{25}FN_2O_2$ m/z: $[M + H]^+$, 369.1973; found, 369.1973.

***N*-(Benzofuran-2-ylmethyl)-*N*′-(3′-(2″-fluoroethoxy)benzyl)-piperazine (29).** The treatment of phenol **20** with 2-fluoroethyl tosylate (**23**) according to the method described above afforded the title compound as a golden oil (265 mg, 72%); R_f 0.19 (hexanes:EtOAc, 50:50). ^{1}H NMR (300 MHz, $CDCl_3$): δ 2.56 (8H, br s), 3.50 (2H, s), 3.70 (2H, s), 4.14−4.26 (2H, dt, J = 4.1 Hz, J = 28 Hz,), 4.64−4.83 (2H, dt, J = 4.2 Hz, J = 47 Hz), 6.58 (1H, s), 6.81 (1H, d, J = 7.2 Hz), 6.90−6.91 (2H, m), 7.17−7.25 (3H, m), 7.49 (2H, dd, J = 7.2, 7.6 Hz). ^{13}C NMR (75.5 MHz, $CDCl_3$): δ 52.9, 53.1, 55.5, 62.9, 67.0, 67.3, 80.9, 83.2, 105.9, 111.4, 113.4, 115.5, 120.8, 122.3, 122.8, 124.0, 128.4, 129.4, 139.9, 154.6, 158.6. HRMS (+ESI) calcd for $C_{22}H_{25}FN_2O_2$ m/z: $[M + H]^+$, 369.1973; found, 369.1929.

***N*-(Benzofuran-2-ylmethyl)-*N*′-(4′-(2″-fluoroethoxy)benzyl)-piperazine (30).** The treatment of phenol **21** with 2-fluoroethyl tosylate (**23**) according to the method described above afforded the title compound as a yellow solid (230 mg, 60%); mp 76−78 °C; R_f 0.25 (hexanes:EtOAc, 50:50). ^{1}H NMR (300 MHz, $CDCl_3$): δ 2.54 (8H, br s), 3.45 (2H, s), 3.69 (2H, s), 4.10−4.28 (2H, dt, J = 4.1 Hz, J = 28 Hz,), 4.60−4.88 (2H, dt, J = 4.1 Hz, J = 47 Hz), 6.57 (1H, s), 6.86 (2H, d, J = 8.5 Hz), 7.19−7.25 (4H, m), 7.50 (2H, d, J = 7.3 Hz). ^{13}C NMR (75.5 MHz, $CDCl_3$): δ 52.4, 52.7, 55.1, 62.0, 72.9, 82.8, 105.4, 111.0, 114.1, 120.4, 122.3, 123.4, 127.3, 130.2, 132.8, 154.2, 154.8, 158.9. MS (+ESI) m/z: 337.27 ($[M + H]^+$, 100%). Anal. ($C_{22}H_{25}FN_2O_2$) calcd: C, 71.72; H, 6.84; N, 7.60. Found: C, 71.49; H, 7.10; N, 7.60.

***N*-(Benzofuran-2-ylmethyl)-*N*′-(2′-propoxybenzyl)piperazine (31).** The treatment of phenol **19** with propyl tosylate (**24**) according to the method described above afforded the title compound as a colorless oil (222 mg, 61%); R_f 0.26 (hexanes:EtOAc, 80:20). ^{1}H NMR (300 MHz, $CDCl_3$): δ 1.03 (3H, t, J = 7.4 Hz), 1.79 (2H, q, J = 6.8 Hz), 2.59 (8H, br s), 3.61 (2H, s), 3.71 (2H, s), 3.90 (2H, t, J = 6.4 Hz), 6.59 (1H, s), 6.74−6.98 (2H, m), 7.13−7.32 (4H, m), 7.45−7.54 (2H, m). ^{13}C NMR (75.5 MHz, $CDCl_3$): δ 10.9, 22.9, 52.8, 53.3, 55.6, 61.5, 69.7, 105.8, 111.5, 116.2, 119.3, 120.2, 120.8, 122.8, 124.1, 128.2, 128.9, 130.9, 154.2, 154.8, 159.0. HRMS (+ESI) calcd for $C_{23}H_{28}N_2O_2$ m/z: $[M + H]^+$, 365.2224; found, 365.2222.

***N*-(Benzofuran-2-ylmethyl)-*N*′-(3′-propoxybenzyl)piperazine (32).** The treatment of phenol **20** with propyl tosylate (**24**) according to the method described above afforded the title compound as a golden oil (226 mg, 62%); R_f 0.32 (hexanes:EtOAc, 70:30). ^{1}H NMR (300 MHz, $CDCl_3$): δ 1.03 (3H, t, J = 7.4 Hz), 1.79 (2H, q, J = 7.0 Hz), 2.56 (8H, br s), 3.49 (2H, s), 3.70 (2H, s), 3.90 (2H, t, J = 6.8 Hz), 6.58 (1H, s), 6.78 (1H, d, J = 7.3 Hz), 6.86 (2H, br s), 7.16−7.26 (3H, m), 7.46 (1H, d, J = 7.5 Hz), 7.51 (1H, d, J = 7.8 Hz). ^{13}C NMR (75.5 MHz, $CDCl_3$): δ 10.7, 22.8, 53.0, 53.1, 55.5, 63.0, 69.6, 105.8, 111.4, 113.2, 115.5, 120.8, 121.5, 122.7, 124.0, 127.4, 129.2, 141.0, 154.6, 154.9, 157.0. HRMS (+ESI) calcd for $C_{23}H_{28}N_2O_2$ m/z: $[M + H]^+$, 365.2224; found, 365.2223.

***N*-(Benzofuran-2-ylmethyl)-*N*′-(4′-propoxybenzyl)piperazine (33).** The treatment of phenol **21** with *n*-propyl tosylate (**24**) according to the method described above afforded the title compound as a golden yellow oil (218 mg, 60%); R_f 0.29 (hexanes:EtOAc, 70:30). ^{1}H NMR (300 MHz, $CDCl_3$): δ 1.03 (3H, t, J = 8.4 Hz), 1.79 (2H, q, J = 6.9 Hz), 2.67 (8H, br s), 3.60 (2H, s), 3.73 (2H, s), 3.90 (2H, t, J = 6.6 Hz), 6.60 (1H, s), 6.83 (2H, d, J = 8.5 Hz), 7.17−7.28 (4H, m), 7.45 (1H, d, J = 7.7 Hz), 7.51 (1H, d, J = 7.2 Hz), 7.49 (1H, d, J = 7.0 Hz). ^{13}C NMR (75.5 MHz, $CDCl_3$): δ 11.1, 23.1, 52.2, 55.4, 62.0, 70.1, 106.8, 111.9, 114.9, 121.4, 123.3, 124.7, 127.7, 130.2, 131.7, 154.3, 154.6, 158.1. HRMS (+ESI) calcd for $C_{23}H_{28}N_2O_2$ m/z: $[M + H]^+$, 365.2224; found, 365.2223.

***N*-(Benzofuran-2-ylmethyl)-*N*′-(2′-(3″-fluoropropoxy)benzyl)-piperazine (34).** The treatment of phenol **19** with 3-fluoropropyl tosylate (**37**) according to the method described above afforded the title compound as a colorless oil (237 mg, 62%); R_f 0.26 (hexanes:EtOAc, 60:40). ^{1}H NMR (300 MHz, $CDCl_3$): δ 2.08−2.25 (2H, m), 2.59 (8H, br s), 3.59 (2H, s), 3.69 (2H, s), 4.08 (2H, t, J = 6.0 Hz), 4.55−4.75 (2H, dt, J = 5.8 Hz, J = 47 Hz), 6.60 (1H, s), 6.84−6.94 (2H, m), 7.16−7.27 (3H, m), 7.32 (1H, d, J = 7.4 Hz), 7.49 (2H, d, J = 7.5 Hz). ^{13}C NMR (75.5 MHz, $CDCl_3$): δ 30.9, 53.2, 53.6, 56.0, 56.4, 64.2, 80.3, 82.5,

106.3, 119.6, 112.0, 121.1, 121.2, 123.2, 124.4, 126.5, 127.4, 128.8, 131.6, 154.2, 154.8, 159.0. HRMS (+ESI) calcd for $C_{23}H_{27}FN_2O_2$ m/z: $[M + H]^+$, 383.2057; found, 383.2132.

***N*-(Benzofuran-2-ylmethyl)-*N*′-(3′-(3″-fluoropropoxy)benzyl)-piperazine (35).** The treatment of phenol **20** with 3-fluoropropyl tosylate (**37**) according to the method described above afforded the title compound as a golden oil (237 mg, 62%); R_f 0.29 (hexanes:EtOAc, 65:35). ^{1}H NMR (300 MHz, $CDCl_3$): δ 2.02−2.21 (2H, m), 2.55 (8H, br s), 3.46 (2H, s), 3.67 (2H, s), 4.05 (2H, t, J = 6.1 Hz), 4.51−4.71 (2H, dt, J = 5.8 Hz, J = 47 Hz), 6.56 (1H, s), 6.76 (1H, d, J = 7.3 Hz), 6.88 (2H, br s), 7.15−7.25 (3H, m), 7.45 (1H, d, J = 7.7 Hz), 7.49 (1H, d, J = 7.8 Hz). ^{13}C NMR (75.5 MHz, $CDCl_3$): δ 30.9, 52.8, 53.2, 55.4, 63.3, 63.8, 80.1, 82.3, 106.5, 111.9, 116.1, 121.3, 123.2, 124.6, 128.2, 128.8, 131.6, 154.5, 155.6, 156.2. HRMS (+ESI) calcd for $C_{23}H_{27}FN_2O_2$ m/z: $[M + H]^+$, 383.2129; found, 383.2131.

***N*-(Benzofuran-2-ylmethyl)-*N*′-(4′-(3″-fluoropropoxy)benzyl)-piperazine (36).** The treatment of phenol **21** with 3-fluoropropyl tosylate (**37**) according to the method described above afforded the title compound as a colorless solid (241 mg, 63%); mp 59−60 °C; R_f 0.24 (hexanes:EtOAc, 50:50). ^{1}H NMR (300 MHz, $CDCl_3$): δ 2.07−2.24 (2H, m), 2.55 (8H, br s), 3.45 (2H, s), 3.69 (2H, s), 4.25 (2H, t, J = 6.1 Hz), 4.54−4.74 (2H, dt, J = 5.8 Hz, J = 47 Hz), 6.58 (1H, s), 6.84 (2H, d, J = 8.4 Hz), 7.17−7.24 (4H, m), 7.49 (2H, d, J = 7.1 Hz). ^{13}C NMR (75.5 MHz, $CDCl_3$): δ 31.9, 52.9, 53.1, 55.6, 62.5, 63.7, 80.0, 105.8, 111.4, 114.3, 120.8, 122.7, 124.0, 127.3, 130.6, 132.2, 154.6, 158.2. MS (+ESI) m/z: 383.33 ($[M + H]^+$, 100%). Anal. ($C_{23}H_{27}FN_2O_2$) calcd: C, 72.23; H, 7.12; N, 7.22. Found: C, 72.56; H, 7.22; N, 7.38.

Radioligand Binding Assay. Affinities for σ_1 were determined using rat brain homogenates and [^{3}H](+)-pentazocine, and affinities for σ_2 were determined using PC12 cells and [^{3}H]DTG using a modification of the protocol reported by Kovacs and Larson.[74] Binding to all receptors were performed by NIMH PDSP, and conditions can be found in the PDSP handbook. Binding data not shown in Tables 1−3 can be found in the Supporting Information.

Lipophilicity Estimations. The lipophilicity of piperazine **13** was examined by determination of the log D value using a HPLC method previously described.[76,77] Phosphate buffer (0.05 M) was prepared by dissolved weighed amounts of potassium dihydrogen phosphate in Alpha-Q water, and the pH was adjusted to 7.4 with sodium hydroxide solution (0.1 M). Samples were analyzed using a MS C-18 column (Waters XTerra, 5 μm, 2.1 mm i.d. × 150 mm) and a mobile phase of methanol and phosphate buffer (65:35 v/v, pH 7.47) with a flow rate of 0.3 mL/min, UV at 254 nm. The lipophilicity of piperazine **13** was estimated by a comparison of its retention time to that of standards having known log D values. The standards used were aniline, benzene, toluene, cumene, triphenylamine, and hexachlorobenzene, prepared as solutions in methanol. All sample injections were performed in triplicate, and the results were averaged to provide the final values. A calibration curve of log D versus retention time was produced, which resulted in an exponential calibration equation ($y = 0.7981e^{0.7371x}$) with an r^2 value 0.992. The exponential equation of the trendline function from the calibration graph and Excel allowed the log D values to be calculated.

Radiochemistry. Preparation of [^{11}C]CH_3I. The target gas (^{14}N + 0.5% $^{16}O_2$) was bombarded with protons using a 16 MeV cyclotron to produce [^{11}C]CO_2. The [^{11}C]CO_2 was transferred to a GE Microlab automated module and concentrated onto molecular sieves. The sieves were heated to release [^{11}C]CO_2, which was reduced by hydrogen on a nickel catalyst to form [^{11}C]CH_4. The [^{11}C]CH_4 was released into the CH_3I conversion part of the module where it was recirculated through a quartz column (packed with ascarite and iodine crystals) by helium carrier gas. The [^{11}C]CH_3I was trapped in ascarite, while any unconverted [^{11}C]CH_4 was transferred to waste.

Preparation and Formulation of 1-(Benzofuran-2-ylmethyl)-4-(4-[^{11}C]methoxybenzyl) Piperazine ([^{11}C]13). Under a helium gas flow, synthesized [^{11}C]CH_3I was delivered to a 1 mL reaction vessel containing **21** (phenol, 0.5 mg, 1.5 μmol) in DMF (300 μL) and TBAH (1.8 μmol) and allowed to stand at RT for 2 min and then heated at 80 °C for 5 min. The reaction mixture was diluted with 0.5 mL of a 0.1 M NaH_2PO_4−CH_3CN (70:30 v/v) solution and injected onto an HPLC XTerra RP C-18 (7.8 mm i.d. × 100 mm, 5 μm particle size) semipreparative reverse phase column. Using a mobile phase of 0.1 M NaH_2PO_4−CH_3CN (70:30 v/v) and a flow rate of 6.0 mL/min, the retention time (t_R) of [^{11}C]**13** was 5.10 min. The radioactive fraction corresponding to [^{11}C]**13** was collected and evaporated under vacuum. The residue was reconstituted in sterile saline (3 mL) and filtered through a sterile Millipore GS 0.22 μm filter into a sterile pyrogen-free evacuated vial.

Quality Control for [^{11}C]13. For the determination of specific radioactivity and radiochemical purity, an aliquot of the final solution of known volume and radioactivity was injected onto an analytical reverse-phase HPLC column (Waters XTerra RP C-18, 4.6 mm × 150 mm). A mobile phase of 0.1 M NaH_2PO_4−CH_3CN (50:50 v/v) at a flow rate of 1.0 mL/min was used to elute [^{11}C]**13** (t_R = 5.10 min). The area of the UV absorbance peak measured at 254 nm corresponding to the carrier product was measured (integrated) on the HPLC chromatogram and compared to a standard curve relating mass to UV absorbance.

PET Studies. Animals. A healthy male *P. hamadryas* baboon that was 13 years old and weighed 26.5 kg was selected for PET scanning. The baboon was maintained and handled in accordance with the National Health and Medical Research Council (NHMRC) code of practice for the care and use of nonhuman primates for scientific purposes. Project application was approved by the Sydney South West Health Service Animal Ethics Committee.

Baboon Carbon-11 PET Imaging. All PET data were acquired using a Siemens Biography LSO PET-CT scanner in the Department of PET and Nuclear Medicine at Royal Prince Alfred Hospital. These dual modality devices have a fully 3D PET scanner with 24 crystal rings and a dual slice CT scanner in the same gantry. These scanners yield a reconstructed PET spatial resolution of 6.3 mm FWDH (full width at half-maximum) in the center of the field of view. A CT scan of the head was completed prior to radioligand injection. The baboon was initially anaesthetized with ketamine (8 mg/kg, im) in addition to medetomidine hydrochloride (Domitor, 30 μg/kg, im). Anaesthesia was maintained with the use of an iv infusion of ketamine in saline at a dose rate of 0.2 mg ketamine/kg/min. The baboon also received $MgSO_4$ (2 mL, iv) given over half an hour and atropine (1 mg, im) plus metoclopramide (Maxolon; Mayne Pharma, 5 mg, im). The head of the baboon was immobilized with plastic tape to minimize motion artifacts. Acquisition of dynamic PET data (20 × 30 s, 30 × 60 s, and 4 × 300 frames) was commenced just prior to radioligand injection and yielded a total of 54 frames over a period of 60 min. The dynamic 3D PET sinograms were rebinned using FORE (Fourier rebinning) and reconstructed into 47 transversal slices with filtered back projection and CT data-based corrections for photon attenuation and scatter, each comprising of 128 × 128 voxels. Reconstructed voxel values in each frame are reported in units of Bq/mL, corrected for radioactive decay to the time of injection, and voxel dimensions were 0.206 cm × 0.206 cm × 0.337 cm. Voxel values were then converted to units of percentage injected dose per volume of brain tissue (% dose/mL) and plotted against time. An automated 3D registration algorithm was used to coregister the two reconstructed scans prior to region of interest definition. Decay-corrected time−activity curves representing the variation on radioligand concentration versus time were constructed from selected slices of region of interest over the whole brain. After dynamic acquisition, a whole body PET-CT scan was performed to determine other sites of uptake of the radioligand.

Blocking Studies. Haloperidol (1 mg/kg) was dissolved in saline with a small quantity of propylene glycol and acetic acid.

Haloperidol was injected iv 5 min prior to tracer injection into the cephalic vein. Drug treatment was separated by at least 3 week intervals.

Acknowledgment. K_i determinations and receptor binding profiles were generously provided by the National Institute of Mental Health's Psychoactive Drug Screening Program, Contract number NO1MH32004 (NIMH PDSP). The NIMH PDSP is directed by Bryan L. Roth M.D., Ph.D., at the University of North Carolina at Chapel Hill and Project Officer Jamie Driscol at NIMH (Bethesda, MD).

Supporting Information Available: Off-target binding data for compounds **10**−**13**, **25**, and **26**. This material is available free of charge via the Internet at http://pubs.acs.org.

References

(1) Martin, W. R.; Eades, C. G.; Thompson, J. A.; Huppler, R. E.; Gilbert, P. E. The effects of morphine- and nalorphine-like drugs in the nondependent and morphine-dependent chronic spinal dog. *J. Pharmacol. Exp. Ther.* **1976**, *197*, 517–532.

(2) Quirion, R.; Chicheportiche, R.; Contreras, P. C.; Johnson, K. M.; Lodge, D.; Tam, S. W.; Woods, J. H.; Zukin, S. R. Classification and nomenclature of phencyclidine and sigma receptor sites. *Trends Neurosci. (Pers. Ed.)* **1987**, *10*, 444–446.

(3) Quirion, R.; Bowen, W. D.; Itzhak, Y.; Junien, J. L.; Musacchio, J. M.; Rothman, R. B.; Su, T. P.; Tam, S. W.; Taylor, D. P. A proposal for the classification of sigma binding sites. *Trends Pharmacol. Sci.* **1992**, *13*, 85–86.

(4) Hanner, M.; Moebius, F. F.; Flandorfer, A.; Knaus, H. G.; Striessnig, J.; Kempner, E.; Glossmann, H. Purification, molecular cloning, and expression of the mammalian sigma1-binding site. *Proc. Natl. Acad. Sci. U.S.A.* **1996**, *93*, 8072–8077.

(5) Kekuda, R.; Prasad, P. D.; Fei, Y. J.; Leibach, F. H.; Ganapathy, V. Cloning and functional expression of the human type 1 sigma receptor (hSigmaR1). *Biochem. Biophys. Res. Commun.* **1996**, *229*, 553–558.

(6) Colabufo, N. A.; Berardi, F.; Abate, C.; Contino, M.; Niso, M.; Perrone, R. Is the sigma2 receptor a histone binding protein? *J. Med. Chem.* **2006**, *49*, 4153–4158.

(7) Abate, C.; Elenewski, J.; Niso, M.; Berardi, F.; Colabufo, N. A.; Azzariti, A.; Perrone, R.; Glennon, R. A. Interaction of the $sigma_2$ Receptor Ligand PB28 with the Human Nucleosome: Computational and Experimental Probes of Interaction with the H2A/H2B Dimer. *ChemMedChem* **2010**, *5*, 268–273.

(8) Su, T. P.; London, E. D.; Jaffe, J. H. Steroid binding at sigma receptors suggests a link between endocrine, nervous, and immune systems. *Science* **1988**, *240*, 219–221.

(9) Monnet, F. P.; Maurice, T. The sigma1 protein as a target for the non-genomic effects of neuro(active)steroids: molecular, physiological, and behavioral aspects. *J. Pharmacol. Sci.* **2006**, *100*, 93–118.

(10) Fontanilla, D.; Johannessen, M.; Hajipour, A. R.; Cozzi, N. V.; Jackson, M. B.; Ruoho, A. E. The Hallucinogen N,N-Dimethyltryptamine (DMT) Is an Endogenous Sigma-1 Receptor Regulator. *Science* **2009**, *323*, 934–937.

(11) Su, T.-P.; Hayashi, T.; Vaupel, D. B. When the endogenous hallucinogenic trace amine N,N-dimethyltryptamine meets the sigma-1 receptor. *Sci. Signal.* **2009**, *2*, pe12.

(12) Hayashi, T.; Rizzuto, R.; Hajnoczky, G.; Su, T.-P. MAM: More than just a housekeeper. *Trends Cell Biol.* **2009**, *19*, 81–88.

(13) Hayashi, T.; Su, T.-P. Sigma-1 receptor chaperones at the ER-mitochondrion interface regulate Ca^{2+} signaling and cell survival. *Cell* **2007**, *131*, 596–610.

(14) Tsai, S.-Y.; Hayashi, T.; Mori, T.; Su, T.-P. Sigma-1 receptor chaperones and diseases. *Cent. Nerv. Syst. Agents Med. Chem.* **2009**, *9*, 184–189.

(15) Hayashi, T.; Maurice, T.; Su, T. P. Ca^{2+} signaling via sigma1-receptors: novel regulatory mechanism affecting intracellular Ca^{2+} concentration. *J. Pharmacol. Exp. Ther.* **2000**, *293*, 788–798.

(16) Lupardus, P. J.; Wilke, R. A.; Aydar, E.; Palmer, C. P.; Chen, Y.; Ruoho, A. E.; Jackson, M. B. Membrane-delimited coupling between sigma receptors and K^+ channels in rat neurohypophysial terminals requires neither G-protein nor ATP. *J. Physiol.* **2000**, *526*, 527–539.

(17) Zhang, H.; Cuevas, J. Sigma receptors inhibit high-voltage-activated calcium channels in rat sympathetic and parasympathetic neurons. *J. Neurophysiol.* **2002**, *87*, 2867–2879.

(18) Aydar, E.; Palmer, C. P.; Klyachko, V. A.; Jackson, M. B. The sigma receptor as a ligand-regulated auxiliary potassium channel subunit. *Neuron* **2002**, *34*, 399–410.

(19) Monnet, F. P. Sigma-1 receptor as regulator of neuronal intracellular Ca^{2+}: clinical and therapeutic relevance. *Biol. Cell* **2005**, *97*, 873–883.

(20) Vilner, B. J.; Bowen, W. D. Modulation of cellular calcium by sigma-2 receptors: release from intracellular stores in human SK-N-SH neuroblastoma cells. *J. Pharmacol. Exp. Ther.* **2000**, *292*, 900–911.

(21) Matsuno, K.; Matsunaga, K.; Senda, T.; Mita, S. Increase in extracellular acetylcholine level by sigma ligands in rat frontal cortex. *J. Pharmacol. Exp. Ther.* **1993**, *265*, 851–859.

(22) Kobayashi, T.; Matsuno, K.; Nakata, K.; Mita, S. Enhancement of acetylcholine release by SA4503, a novel sigma 1 receptor agonist, in the rat brain. *J. Pharmacol. Exp. Ther.* **1996**, *279*, 106–113.

(23) Horan, B.; Gifford, A. N.; Matsuno, K.; Mita, S.; Ashby, C. R., Jr. Effect of SA4503 on the electrically evoked release of ^{3}H-acetylcholine from striatal and hippocampal rat brain slices. *Synapse* **2002**, *46*, 1–3.

(24) Gonzalez-Alvear, G. M.; Werling, L. L. Regulation of [^{3}H]dopamine release from rat striatal slices by sigma receptor ligands. *J. Pharmacol. Exp. Ther.* **1994**, *271*, 212–219.

(25) Gonzalez-Alvear, G. M.; Werling, L. L. sigma1 Receptors in rat striatum regulate NMDA-stimulated [^{3}H]dopamine release via a presynaptic mechanism. *Eur. J. Pharmacol.* **1995**, *294*, 713–719.

(26) Weatherspoon, J. K.; Gonzalez-Alvear, G. M.; Frank, A. R.; Werling, L. L. Regulation of [^{3}H] dopamine release from mesolimbic and mesocortical areas of guinea pig brain by sigma receptors. *Schizophr. Res.* **1996**, *21*, 51–62.

(27) Gonzalez, G. M.; Werling, L. L. Release of [^{3}H]dopamine from guinea pig striatal slices is modulated by sigma1 receptor agonists. *Naunyn-Schmiedeberg's Arch. Pharmacol.* **1997**, *356*, 455–461.

(28) Hayashi, T.; Kagaya, A.; Takebayashi, M.; Shimizu, M.; Uchitomi, Y.; Motohashi, N.; Yamawaki, S. Modulation by sigma ligands of intracellular free Ca++ mobilization by N-methyl-D-aspartate in primary culture of rat frontal cortical neurons. *J. Pharmacol. Exp. Ther.* **1995**, *275*, 207–214.

(29) Debonnel, G.; de Montigny, C. Modulation of NMDA and dopaminergic neurotransmissions by sigma ligands: possible implications for the treatment of psychiatric disorders. *Life Sci.* **1996**, *58*, 721–734.

(30) Bermack, J. E.; Debonnel, G. Modulation of serotonergic neurotransmission by short- and long-term treatments with sigma ligands. *Br. J. Pharmacol.* **2001**, *134*, 691–699.

(31) Lucas, G.; Rymar, V. V.; Sadikot, A. F.; Debonnel, G. Further evidence for an antidepressant potential of the selective sigma1 agonist SA 4503: electrophysiological, morphological and behavioural studies. *Int. J. Neuropsychopharmacol.* **2008**, *11*, 485–495.

(32) Monnet, F. P.; Debonnel, G.; de Montigny, C. In vivo electrophysiological evidence for a selective modulation of N-methyl-D-aspartate-induced neuronal activation in rat CA3 dorsal hippocampus by sigma ligands. *J. Pharmacol. Exp. Ther.* **1992**, *261*, 123–130.

(33) Monnet, F. P.; Mahe, V.; Robel, P.; Baulieu, E. E. Neurosteroids, via sigma receptors, modulate the [^{3}H]norepinephrine release evoked by N-methyl-D-aspartate in the rat hippocampus. *Proc. Natl. Acad. Sci. U.S.A.* **1995**, *92*, 3774–3778.

(34) Monnet, F. P.; de Costa, B. R.; Bowen, W. D. Differentiation of sigma ligand-activated receptor subtypes that modulate NMDA-evoked [^{3}H]-noradrenaline release in rat hippocampal slices. *Br. J. Pharmacol.* **1996**, *119*, 65–72.

(35) Hashimoto, K.; Ishiwata, K. Sigma receptor ligands: Possible application as therapeutic drugs and as radiopharmaceuticals. *Curr. Pharm. Des.* **2006**, *12*, 3857–3876.

(36) Cobos, E. J.; Entrena, J. M.; Nieto, F. R.; Cendán, C. M.; Del Pozo, E. Pharmacology and Therapeutic Potential of Sigma1 Receptor Ligands. *Curr. Neuropharmacol.* **2008**, *6*, 344–366.

(37) Maurice, T.; Su, T.-P. The pharmacology of sigma-1 receptors. *Pharmacol. Ther.* **2009**, *124*, 195–206.

(38) Tam, S. W.; Cook, L. Sigma opiates and certain antipsychotic drugs mutually inhibit (+)-[^{3}H] SKF 10,047 and [^{3}H]haloperidol binding in guinea pig brain membranes. *Proc. Natl. Acad. Sci. U.S.A.* **1984**, *81*, 5618–5621.

(39) Frieboes, R.-M.; Steiger, A. The antipsychotic effects of sigma drugs. In *Neurotransmitter Receptors in Actions of Antipsychotic Medications*; Lidow, M. S., Ed.; CRC Press: Boca Raton, 2000; pp 137−152.

(40) Itzhak, Y.; Kassim, C. O. Clorgyline displays high affinity for sigma binding sites in C57BL/6 mouse brain. *Eur. J. Pharmacol.* **1990**, *176*, 107–108.

(41) Narita, N.; Hashimoto, K.; Tomitaka, S.; Minabe, Y. Interactions of selective serotonin reuptake inhibitors with subtypes of sigma receptors in rat brain. *Eur. J. Pharmacol.* **1996**, *307*, 117–119.
(42) Bermack, J. E.; Debonnel, G. The role of sigma receptors in depression. *J. Pharmacol. Sci.* **2005**, *97*, 317–336.
(43) Hayashi, T.; Stahl, S. M. The sigma-1 (σ_1) receptor and its role in the treatment of mood disorders. *Drugs Future* **2009**, *34*, 137–146.
(44) Kulkarni, S. K.; Dhir, A. σ-1 receptors in major depression and anxiety. *Expert Rev. Neurother.* **2009**, *9*, 1021–1034.
(45) Matsumoto, R. R.; McCracken, K. A.; Pouw, B.; Zhang, Y.; Bowen, W. D. Involvement of sigma receptors in the behavioral effects of cocaine: evidence from novel ligands and antisense oligodeoxynucleotides. *Neuropharmacology* **2002**, *42*, 1043–1055.
(46) Maurice, T.; Martin-Fardon, R.; Romieu, P.; Matsumoto, R. R. Sigma(1) (σ_1) receptor antagonists represent a new strategy against cocaine addiction and toxicity. *Neurosci. Biobehav. Rev.* **2002**, *26*, 499–527.
(47) Matsumoto, R. R.; Liu, Y.; Lerner, M.; Howard, E. W.; Brackett, D. J. Sigma receptors: Potential medications development target for anti-cocaine agents. *Eur. J. Pharmacol.* **2003**, *469*, 1–12.
(48) Nguyen, E. C.; McCracken, K. A.; Liu, Y.; Pouw, B.; Matsumoto, R. R. Involvement of sigma (σ) receptors in the acute actions of methamphetamine: Receptor binding and behavioral studies. *Neuropharmacology* **2005**, *49*, 638–645.
(49) Romieu, P.; Maurice, T. The sigma1 (s1) protein as a new target for anti-cocaine therapy. In *Cocaine and Heroin Abuse Research*; Pizzoli, L. A., Ed.; Nova Science Publishers: Hauppauge, NY, 2006; pp 37−60.
(50) John, C. S.; Bowen, W. D.; Varma, V. M.; McAfee, J. G.; Moody, T. W. Sigma receptors are expressed in human non-small cell lung carcinoma. *Life Sci.* **1995**, *56*, 2385–2392.
(51) Vilner, B. J.; John, C. S.; Bowen, W. D. Sigma-1 and sigma-2 receptors are expressed in a wide variety of human and rodent tumor cell lines. *Cancer Res.* **1995**, *55*, 408–413.
(52) Wang, B.; Rouzier, R.; Albarracin, C. T.; Sahin, A.; Wagner, P.; Yang, Y.; Smith, T. L.; Bernstam, F. M.; Marcelo, A. C.; Hortobagyi, G. N.; Pusztai, L. Expression of sigma 1 receptor in human breast cancer. *Breast Cancer Res. Treat.* **2004**, *87*, 205–214.
(53) Vilner, B. J.; de Costa, B. R.; Bowen, W. D. Cytotoxic effects of sigma ligands: sigma receptor-mediated alterations in cellular morphology and viability. *J. Neurosci.* **1995**, *15*, 117–134.
(54) Moody, T. W.; Leyton, J.; John, C. Sigma ligands inhibit the growth of small cell lung cancer cells. *Life Sci.* **2000**, *66*, 1979–1986.
(55) Berthois, Y.; Bourrie, B.; Galiegue, S.; Vidal, H.; Carayon, P.; Martin, P. M.; Casellas, P. SR31747A is a sigma receptor ligand exhibiting antitumoural activity both in vitro and in vivo. *Br. J. Cancer* **2003**, *88*, 438–446.
(56) Crawford, K. W.; Bowen, W. D. Sigma-2 receptor agonists activate a novel apoptotic pathway and potentiate antineoplastic drugs in breast tumor cell lines. *Cancer Res.* **2002**, *62*, 313–322.
(57) Aydar, E.; Palmer, C. P.; Djamgoz, M. B. Sigma receptors and cancer: Possible involvement of ion channels. *Cancer Res.* **2004**, *64*, 5029–5035.
(58) Wheeler, K. T.; Wang, L. M.; Wallen, C. A.; Childers, S. R.; Cline, J. M.; Keng, P. C.; Mach, R. H. Sigma-2 receptors as a biomarker of proliferation in solid tumours. *Br. J. Cancer* **2000**, *82*, 1223–1232.
(59) Collier, T. L.; Waterhouse, R. N.; Kassiou, M. Imaging sigma receptors: Applications in drug development. *Curr. Pharm. Des.* **2007**, *13*, 51–72.
(60) Glennon, R. A.; Ablordeppey, S. Y.; Ismaiel, A. M.; el-Ashmawy, M. B.; Fischer, J. B.; Howie, K. B. Structural features important for sigma 1 receptor binding. *J. Med. Chem.* **1994**, *37*, 1214–1219.
(61) Ablordeppey, S. Y.; Fischer, J. B.; Glennon, R. A. Is a nitrogen atom an important pharmacophoric element in sigma ligand binding? *Bioorg. Med. Chem.* **2000**, *8*, 2105–2111.
(62) Ablordeppey, S. Y.; Fischer, J. B.; Law, H.; Glennon, R. A. Probing the proposed phenyl-A region of the sigma-1 receptor. *Bioorg. Med. Chem.* **2002**, *10*, 2759–2765.
(63) Glennon, R. A. Pharmacophore identification for sigma-1 (σ_1) receptor binding: application of the "deconstruction-reconstruction-elaboration" approach. *Mini Rev. Med. Chem.* **2005**, *5*, 927–940.
(64) Cratteri, P.; Romanelli, M. N.; Cruciani, G.; Bonaccini, C.; Melani, F. GRIND-derived pharmacophore model for a series of alpha-tropanyl derivative ligands of the sigma-2 receptor. *J. Comput.-Aided Mol. Des.* **2004**, *18*, 361–374.
(65) Abate, C.; Mosier, P. D.; Berardi, F.; Glennon, R. A. A Structure-Affinity and Comparative Molecular Field Analysis of Sigma-2 (σ_2) Receptor Ligands. *Cent. Nerv. Syst. Agents Med. Chem.* **2009**, *9*, 246–257.
(66) Laurini, E.; Zampieri, D.; Mamolo, M. G.; Vio, L.; Zanette, C.; Florio, C.; Posocco, P.; Fermeglia, M.; Pricl, S. A 3D-pharmacophore model for σ_2 receptors based on a series of substituted benzo-[d]oxazol-2(3H)-one derivatives. *Bioorg. Med. Chem. Lett.* **2010**, *20*, 2954–2957.
(67) Banister, S. D.; Moussa, I. A.; Jordan, M. J. T.; Coster, M. J.; Kassiou, M. Oxo-bridged isomers of aza-trishomocubane sigma (σ) receptor ligands: Synthesis, in vitro binding, and molecular modeling. *Bioorg. Med. Chem. Lett.* **2010**, *20*, 145–148.
(68) Liu, X.; Banister, S. D.; Christie, M. J.; Banati, R.; Meikle, S.; Coster, M. J.; Kassiou, M. Trishomocubanes: Novel sigma ligands modulate cocaine-induced behavioural effects. *Eur. J. Pharmacol.* **2007**, *555*, 37–42.
(69) Baziard-Mouysset, G.; Younes, S.; Labssita, Y.; Payard, M.; Caignard, D.-H.; Rettori, M.-C.; Renard, P.; Pfeiffer, B.; Guardiola-Lemaitre, B. Synthesis and structure-activity relationships of novel 2-amino alkyl chromones and related derivatives as s site-selective ligands. *Eur. J. Med. Chem.* **1998**, *33*, 339–347.
(70) Younes, S.; Labssita, Y.; Baziard-Mouysset, G.; Payard, M.; Rettori, M.; Renard, P.; Pfeiffer, B.; Caignard, D. Synthesis and structure-activity relationships of novel arylalkyl 4-benzyl piperazine derivatives as sigma site selective ligands. *Eur. J. Med. Chem.* **2000**, *35*, 107–121.
(71) Löwik, D. W. P. M.; Lowe, C. R. Synthesis of Macrocyclic, Triazine-Based Receptor Molecules. *Eur. J. Org. Chem.* **2001**, *2001*, 2825–2839.
(72) Carpino, L. A.; Mansour, E. M. E.; Cheng, C. H.; Williams, J. R.; MacDonald, R.; Knapczyk, J.; Carman, M.; Lopusinski, A. Polystyrene-based deblocking-scavenging agents for the 9-fluorenylmethyloxycarbonyl amino-protecting group. *J. Org. Chem.* **1983**, *48*, 661–665.
(73) Tahtaoui, C.; Parrot, I.; Klotz, P.; Guillier, F.; Galzi, J.-L.; Hibert, M.; Ilien, B. Fluorescent Pirenzepine Derivatives as Potential Bitopic Ligands of the Human M1Muscarinic Receptor. *J. Med. Chem.* **2004**, *47*, 4300–4315.
(74) Kovacs, K. J.; Larson, A. A. Up-regulation of [^{3}H]DTG but not [^{3}H](+)-pentazocine labeled sigma sites in mouse spinal cord by chronic morphine treatment. *Eur. J. Pharmacol.* **1998**, *350*, 47–52.
(75) Eckleman, W. C. The Design of Site-Directed Radiopharmaceuticals for Use in Drug Discovery. In *Nuclear Imaging in Drug Discovery, Development and Approval*; Burns, D. H., Gibson, R. E., Dannals, R. F., Siegl, P. K., Eds.; Birkhäuser: Boston, 1993; pp 113−134.
(76) Quinlivan, M.; Mattner, F.; Papazian, V.; Zhou, J.; Katsifis, A.; Emond, P.; Chalon, S.; Kozikowski, A.; Guilloteau, D.; Kassiou, M. Synthesis and evaluation of iodine-123 labelled tricyclic tropanes as radioligands for the serotonin transporter. *Nucl. Med. Biol.* **2003**, *30*, 741–746.
(77) Waterhouse, R. N.; Mardon, K.; Giles, K. M.; Collier, T. L.; O'Brien, J. C. Halogenated 4-(phenoxymethyl)piperidines as potential radiolabeled probes for sigma-1 receptors: in vivo evaluation of [^{123}I]-1-(iodopropen-2-yl)-4-[(4-cyanophenoxy)methyl]-piperidine. *J. Med. Chem.* **1997**, *40*, 1657–1667.
(78) Walker, J. M.; Bowen, W. D.; Goldstein, S. R.; Roberts, A. H.; Patrick, S. L.; Hohmann, A. G.; DeCosta, B. Autoradiographic distribution of [^{3}H](+)-pentazocine and [^{3}H]1,3-di-o-tolylguanidine (DTG) binding sites in guinea pig brain: a comparative study. *Brain Res.* **1992**, *581*, 33–38.
(79) Bouchard, P.; Quirion, R. [^{3}H]1,3-di(2-tolyl)guanidine and [^{3}H](+)pentazocine binding sites in the rat brain: autoradiographic visualization of the putative sigma1 and sigma2 receptor subtypes. *Neuroscience* **1997**, *76*, 467–477.
(80) Honer, M.; Bruhlmeier, M.; Missimer, J.; Schubiger, A. P.; Ametamey, S. M. Dynamic Imaging of Striatal D2 Receptors in Mice Using Quad-HIDAC PET. *J. Nucl. Med.* **2004**, *45*, 464–470.
(81) Kawamura, K.; Ishiwata, K.; Shimada, Y.; Kimura, Y.; Kobayashi, T.; Matsuno, K.; Homma, Y.; Senda, M. Preclinical evaluation of [^{11}C]SA4503: Radiation dosimetry,in vivo selectivity and PET imaging of sigma1 receptors in the cat brain. *Ann. Nucl. Med.* **2000**, *14*, 285–292.
(82) Yousef, K. A.; Fowler, J. S.; Volkow, N. D.; Dewey, S. L.; Shea, C.; Schlyer, D. J.; Gatley, S. J.; Logan, J.; Wolf, A. P. [^{18}F]haloperidol binding in baboon brain in vivo. *Nucl. Med. Biol.* **1996**, *23*, 47–52.
(83) Yousef, K. A.; Volkow, N. D.; Schlyer, D. J.; Fowler, J. S.; Wolf, A. P.; Wang, G.-J.; Smith, M. R.; Brodie, J. D.; Warner, D. Haloperidol blocks the uptake of [^{18}F]N-methylspiroperidol by extrastriatal dopamine receptors in schizophrenic patients. *Synapse* **1995**, *19*, 14–17.
(84) Kabalka, G. W.; Varma, M.; Varma, R. S.; Srivastava, P. C.; Knapp, F. F. The tosylation of alcohols. *J. Org. Chem.* **1986**, *51*, 2386–2388.
(85) Parenty, A. D. C.; Smith, L. V.; Cronin, L. An unusual substitution reaction directed by an intramolecular re-arrangement. *Tetrahedron* **2005**, *61*, 8410–8418.